

GIFT: A Framework for Global Interpretable Faithful Textual Explanations of Vision Classifiers

Éloi Zablocki^{*,1}, Valentin Gerard^{*,1}, Amaia Cardiel^{1,2},
Eric Gaussier², Matthieu Cord^{1,3}, Eduardo Valle¹

¹Valeo.ai, France ²Université Grenoble Alpes, France ³Sorbonne Université, France

Abstract

Understanding deep models is crucial for deploying them in safety-critical applications. We introduce GIFT, a framework for deriving post-hoc, global, interpretable, and faithful textual explanations for vision classifiers. GIFT starts from local faithful visual counterfactual explanations and employs (vision) language models to translate those into global textual explanations. Crucially, GIFT provides a verification stage measuring the causal effect of the proposed explanations on the classifier decision. Through experiments across diverse datasets, including CLEVR, CelebA, and BDD, we demonstrate that GIFT effectively reveals meaningful insights, uncovering tasks, concepts, and biases used by deep vision classifiers. Our code, data, and models are released at github.com/valeoai/GIFT.

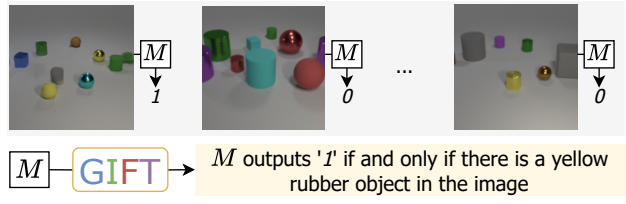
1. Introduction

Understanding how deep vision models make decisions is essential for their practical use, especially in critical applications such as self-driving cars [55, 86] and medical image analysis [72]. Clear, reliable explanations of model decisions are needed to build user trust and ensure effective deployment. In this paper, we focus on *post-hoc* explanations, i.e., generated after model training, in contrast to approaches that add explainability constraints during model design [7, 36, 90]. Post-hoc explainability generally focuses on *local* explanations, which interpret the model’s decision for a specific image, e.g., with saliency maps [23, 66, 69] or counterfactual explanations [40, 42, 75, 88]. Local explanations, however, offer little insights about how the model behaves overall, across a range of inputs. That is the goal of *global* explanations, which target a holistic understanding of the model [21, 22, 48, 49].

Explanations must also be *interpretable* to be useful for humans [29]: fully understandable and intuitively meaningful. Representations that fall short of that goal include

^{*}equal contribution

Use-case 1: Uncovering classification rules



Use-case 2: Fine-grained concept discovery



Use-case 3: Automatic model bias discovery

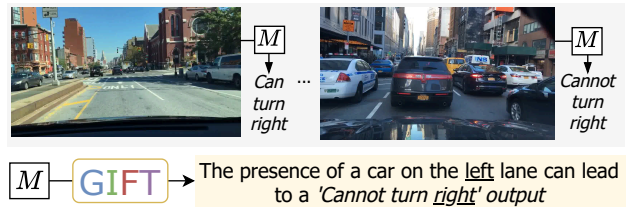


Figure 1. **Illustration of use-cases that GIFT can address.** Given a trained image classifier M , GIFT globally explains the model in natural language: it can uncover unknown class meaning (1), discover fine-grained relationships between data features and classification outcomes (2), and find unexpected biases (3).

the saliency maps of input attribution [8, 19, 23, 66, 69, 76, 87, 92], the image pairs of counterfactual explanations [40–43, 59, 63, 75, 88], and the disentangled directions in latent neural-network space of concept-based methods [21, 22, 46, 48, 49, 91], all of which requiring either subjective interpretation, hand-labeling [20], or both.

Additionally, explanations must be *faithful*, accurately representing the model’s decision-making [14, 65]. Many

methods, including model-agnostic approaches [52, 62] and concept-based methods [21, 22, 46, 48, 49, 91] produce explanations that capture correlations rather than causal associations, which risks misleading end-users.

In this work, we introduce GIFT, a novel framework to obtain Global, Interpretable, Faithful, and Textual explanations for deep vision models. GIFT starts with faithful local explanations for the model using counterfactual explanations [42, 75, 88], which reveal minimal meaningful changes in an input leading the model to change its output. GIFT exploits natural language both to make the explanations directly *interpretable* for end-users and to enable processing by Large Language Models (LLMs) [44, 54], which can summarize large amounts of text and have recently achieved significant advances in reasoning. That strategy allows obtaining *global interpretable* explanations. Crucially, GIFT proposes a verification of the candidate explanations, allowing measuring their causal effect [30, 58] through interventions on the input using image-editing models.

We demonstrate the usefulness of GIFT across three experimental use cases (Figure 1). First, we demonstrate GIFT uncovering classification rules, in models trained on the CLEVR dataset [45], which allows controlled experiments with complex compositionality. Second, we showcase the power of GIFT to guide the exploration for detailed explanations in a less controlled scenario, using the CelebA [51] dataset. Finally, we use GIFT to identify biases on a classifier trained on the BDD-OIA [85] dataset, a challenging domain with complex driving scenes.

Overall, our contributions are as follows:

- We introduce GIFT, the first automated framework for global, faithful, explicitly interpretable explanations for vision classifiers.
- We derive global explanations by combining two ideas: (1) gathering counterfactual signals across the model’s input domain, which are inherently causal although very local; and (2) reasoning with an LLM to uncover global insights from those local signals. Both ideas and their combined synergy are novel, to our knowledge.
- GIFT comes with explanation verification tools, measuring both correlation and causal association. It allows end-users to interact with its output to understand the target classifier further.
- We demonstrate GIFT’s ability to generate accurate, meaningful, global explanations across various datasets and use cases.

2. Related Work

Literature generally categorizes explainability methods as either *intrinsic* [7, 11, 36, 90], designed during the model-building phase to create inherently interpretable models, or *post-hoc*, which probe trained models to provide insight into their decisions [11, 36, 90]. Post-hoc methods are fur-

ther divided into *local*, which focus on explaining individual predictions, and *global*, which aim to capture broader patterns of model behavior across the data domain.

Input Attribution Methods. Input attribution techniques aim to highlight regions of the input image that most influence the model’s predictions, often visualized as a saliency map. Common strategies include gradient-based methods [8, 19, 66, 69, 87, 92], which back-propagate gradients to identify influential features, and perturbation-based methods that remove or alter parts of the input to observe resulting changes in model output [23, 76]. However, attribution maps can only provide local explanations for each instance. They require user interpretation, introducing subjective biases [9], and are sometimes unreliable as they can mislead end-users by acting as edge detectors [2].

Model-Agnostic Methods. Model-agnostic methods explain black-box models through interpretable surrogate models. Approaches like LIME [62] and SHAP [52] are widely used to provide *local* explanations, with some attempts at *global* surrogates for more holistic interpretability [25, 34, 89, 93]. The simplification techniques these methods employ, such as using superpixels [62] or high-level input features [52], can result in reduced fidelity to the model’s original decision process, which may diminish the reliability of explanations for complex, high-dimensional data.

Counterfactual Explanations. Counterfactual explanations are images minimally altered to yield a different classification outcome, thus revealing semantic changes needed to cross the classifier’s decision boundary [75]. Retrieval-based [31, 37, 74, 77] and generator-based methods — with GAN [40, 47, 63, 88] or diffusion models [5, 41, 42, 67] — are used to create realistic counterfactuals. While counterfactuals can provide intuitive insights, they are inherently local explanations. Moreover, they demand careful user interpretation, which may introduce human biases [9, 88].

Concept-Based Explanations. Concept-based methods explain model decisions using human-interpretable ‘concepts’ [48, 50]. They range from neuron-level analyses [6, 27] to layer-level analyses, such as ‘Concept Activation Vectors’ (CAV) [48]. Generally, concept-based methods require annotated data that signals concept presence or absence [48], with some exceptions [28]. Some methods decompose activation patterns using matrix factorization, extracting primary CAV directions [22, 46, 49, 91]. Concept-based explanations usually require model architecture details and weights, which may not be accessible and are often architecture-specific, with most methods only supporting CNN-based models [22, 46, 49]. Additionally, manually

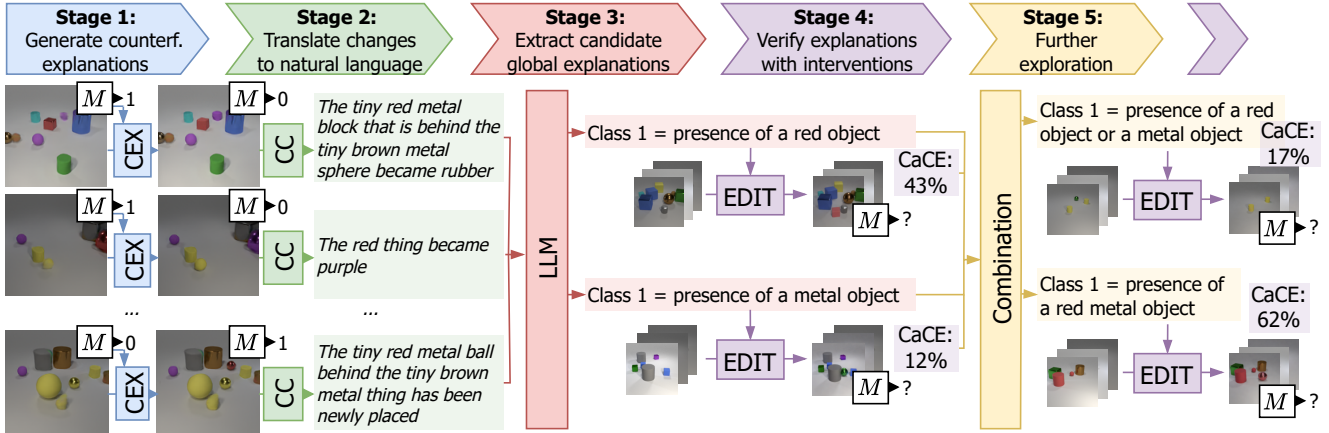


Figure 2. **Overview of GIFT.** For a target model M , here a classifier discriminating images with a ‘red metal object’, GIFT involves five stages: (1) generating local visual counterfactual explanations for several images, the counterfactuals reveal semantic and minimal changes to the query image that flip the classifier’s output, (2) using an image change captioning model to translate in natural language the visual differences between original and counterfactual images, (3) applying an LLM to identify and summarize common patterns from local explanations, thereby proposing candidate global explanations, (4) validating these candidate explanations with intervention studies, and (5) exploring explanation combinations and measuring their validity (using the metrics of stage 4).

defined concepts can miss model biases, while unsupervised concepts [22, 28] require further visualization [20] and human interpretation. In contrast, GIFT identifies explanations grounded in counterfactual signals, bypassing the need for predefined concept annotations and avoiding the introduction of prior on what the model might be using. Moreover, the generated textual explanations are directly interpretable and can be tested for faithfulness, enabling a more reliable insight than correlation-only approaches.

Error Explanations with Language. Language-based approaches have been used to identify model corner cases and errors. Some frameworks rely on textual inputs from users [1, 13] or from LLMs [59, 79] to diagnose weaknesses; however, this can introduce bias and restrict the scope of potential findings, as it uses prior knowledge about the error types to look for. In contrast, GIFT uses an LLM as a summarizing tool of counterfactual-based analysis rather than as a knowledge base, which limits the introduction of LLM-based bias. Other works [18, 81] identify subsets of data where systematic errors occur and then label them. Unlike these methods, which usually rely on ground-truth labels for error analysis, our approach extends beyond failure analysis to explain both correct and incorrect classifications, allowing for a unified understanding of model behavior across all outcomes.

3. GIFT Framework

GIFT automatically identifies and validates explanations for a differentiable target classifier M . An **explanation**, here, is an interpretable description of features, attributes, or con-

cepts in input images that are significant to the classifier’s decision. Explanations should be meaningful to humans and faithful to the classifier’s behavior.

3.1. Overview

The proposed approach works as follows (Figure 2). In Stage 1 (Section 3.2), GIFT creates local explanations by generating various counterfactual pairs of images, highlighting faithful visual features relevant to M ’s decision at the individual input level. In Stage 2 (Section 3.3), GIFT uses a Vision Language Model (VLM) to translate the differences between each image in a counterfactual pair into interpretable text descriptions. In Stage 3 (Section 3.4), GIFT employs an LLM to identify recurrent patterns on those local explanations to obtain global candidate explanations that aim to reflect the classifier’s general behavior. In Stage 4 (Section 3.5), we evaluate those candidate explanations on correlation and causal metrics, measuring whether they faithfully reflect M ’s decision process. Finally, in Stage 5 (Section 3.6), we explore the explanation space, combining the rules found so far and using the metrics of Stage 4 to validate our explanation.

3.2. Stage 1: Faithful visual and local explanations

sec:model:counterfactual

GIFT starts by generating local, faithful visual explanations using counterfactual explanation methods [42, 88], which find minimal modifications on input images to flip the model’s decisions. Contrarily to adversarial attacks [70], counterfactual techniques strive to be semantically meaningful [24]. They reveal, locally, the model’s semantic decision boundaries.

Concretely, for our target model M and each image x in a sample set \mathcal{I} of size N , we use a counterfactual explanation method CEX to produce a counterfactual image x' , with the model decision $M(x') \neq M(x)$. That results in a set of image pairs $\mathcal{P} = \{(x, x') | x \in \mathcal{I}, x' = \text{CEX}(x, M(x), M)\}$, from which later stages will identify meaningful features. Remark that CEX takes into account the input image x , the model decision $M(x)$, which CEX aims to flip, *and directly the model M* , e.g., by considering the model weights. That allows CEX to provide a counterfactual faithful to M , although local to the input x .

3.3. Stage 2: From visual counterfactuals to text

For each counterfactual pair, GIFT creates a change caption, translating the visual changes from the original image to the counterfactual into simple, descriptive natural language.

Visual counterfactuals, *per se*, require a time-consuming and subjective manual comparison to become interpretable. We use instead vision-language models (VLMs) to *change-caption* [4, 32, 38, 60] each image pair, i.e., to automatically describe the changes between each original image x and its counterfactual x' .

Concretely, we employ a Change Captioning model CC that inputs the pair of images and outputs a change caption $t = \text{CC}(x, x')$. At this stage, our explanations have gained in interpretability since an explicitly stated change caption is more interpretable than the implicit changes in an image pair. The explanations are still very local (to each image pair) and may be less faithful since text is a much more compressed representation than images, and the VLM may introduce other forms of noise. We address those challenges next.

3.4. Stage 3: Candidate global explanations

GIFT will now gather all change captions, analyze them for recurrent patterns, and propose candidate global explanations for the target model behavior.

Concretely, we gather the set of all local explanation tuples $\mathcal{T} = \{(\text{CC}(x, x'), M(x), M(x')) | (x, x') \in \mathcal{P}\}$ and use an LLM to summarize them into a set of candidate global explanations $\mathcal{E} = \text{LLM}(\mathcal{T})$ that helps explaining the classifier’s behavior. Remark that the LLM has access, for each tuple, to both the change caption and to what happened to the model decision ($M(x) \rightarrow M(x')$). The LLM has no direct access to the model itself.

This stage addresses the shortcomings of the local explanations. It *disambiguates local evidence* where a given counterfactual change implies multiple plausible explanations. For example, a ‘red metal ball became brown’ explanation, in isolation, could mean that the classifier tracks the absence of ‘red objects’ (or ‘red metal objects’) in class 0 or the presence of ‘brown objects’ (or ‘brown metal objects’) in class 1. This stage also *filters out noise*, alleviat-

ing linguistic variations and eliminating most irrelevant or inconsistent explanations raised in Stage 2.

3.5. Stage 4: Hypotheses verification

The initial explanations at Stage 1, although local and laborious to interpret, are faithful. At the end of Stage 3, we have global interpretable explanations but cannot guarantee their faithfulness, as the VLM and LLM may introduce noise and hallucinations.

Stage 4, therefore, will verify which explanations in \mathcal{E} remain faithful to the model’s behavior. For each explanation $e \in \mathcal{E}$ (e.g., ‘class 1 implies the presence of a red object’), we derive the underlying concept c_e (e.g., ‘red object’) and use those concepts in a two-step verification.

Coarse filter. This first step measures the **correlation** between the model’s decision and the underlying concept c_e of each candidate explanation $e \in \mathcal{E}$. We use the Directed Information (DI) [26] between the concept c_e and the predicted class label y as the correlation metric:

$$\text{DI}(c_e, y) = \frac{I(c_e; y)}{H(c_e)}, \quad (1)$$

where $I(c_e, y)$ is the mutual information between the concept presence and the classifier output, and $H(c_e)$ is the entropy of the concept presence. DI quantifies how much the explanation e explains the classifier’s decision y , assessing the directional influence of the explanation on the classification outcome. More details about its computation appear in [Section A.1](#).

We use a Visual Question Answering model VQA : $(x, c_e) \rightarrow \{0, 1\}$ to find whether concept c_e appears in the image x . We measure the DI for each explanation, rank them, and keep the most promising for further evaluation. The motivation for this pre-filtering is that applying the VQA model is much easier (and computationally cheaper) than intervening on the images with the edit model.

Fine filter. We evaluate the high-correlation explanations $e \in \mathcal{E}$ that pass the coarse filter on their **causal effect** on the classifier’s decision by measuring the causal association [30, 58] between their underlying concept c_e and the model decision y . We partition the samples of a validation set of images according to c_e , *intervene* on those images by inserting or removing c_e and verify the impact of those interventions on the model decision.

Concretely, we use $\text{VQA}(x, c_e)$ to partition a validation set \mathcal{X} into $\mathcal{X}_{c_e=0}$ and $\mathcal{X}_{c_e=1}$ and an image-editing generative model EDIT to make the intervention and edit x into $\tilde{x} = \text{EDIT}(x, c_e)$, by flipping the presence of c_e in the image. Image editing falls short of the unfeasible ideal of modifying physical reality in past image acquisition and

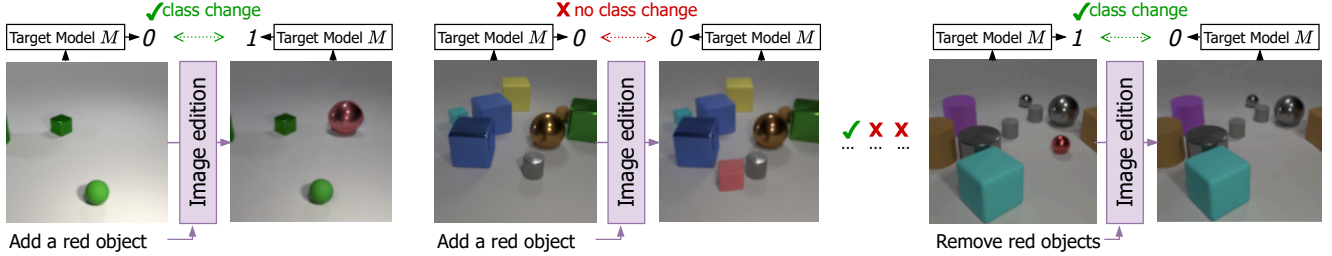


Figure 3. **Causal Concept Effect, CaCE, Stage 4.** For a candidate explanation e (e.g., ‘class 1 implies presence of a red object’), we use an image-editing model to add or remove the underlying concept c_e (e.g., ‘red object’) and observe the impact on the classification outcome, which is aggregated to estimate the CaCE (Eq. 3). In the example, the classifier M recognizes images with a ‘red metal object’, and we observe, as expected, a partial causal effect: removing red objects impacts the outcome, but inserting non-metal red ones does not.

assumes other concepts will be left relatively undisturbed. Nevertheless, this practical procedure has shown good results in estimating the actual causal effect [30].

To measure the impact of the interventions, we create an image $x^{+c_e} = \text{EDIT}(x, c_e)$ for each image $x \in \mathcal{X}_{c_e=0}$, adding the concept c_e (similarly, $\forall x \in \mathcal{X}_{c_e=1}, x^{-c_e} = \text{EDIT}(x, c_e)$). The Individual Causal Effect (ICE) is then

$$\text{ICE}(x) = \begin{cases} M(x^{+c_e}) - M(x) & \forall x \in \mathcal{X}_{c_e=0} \\ M(x) - M(x^{-c_e}) & \forall x \in \mathcal{X}_{c_e=1}, \end{cases} \quad (2)$$

where $M(x)$ is the model decision on input x . Finally, the Causal Concept Effect (CaCE) [30] averages ICE across all images:

$$\text{CaCE}_{c_e \rightarrow y} = \frac{1}{|\mathcal{X}|} \left| \sum_{x \in \mathcal{X}} \text{ICE}(x) \right| \quad (3)$$

For binary classifiers, or multiclass ones evaluated in 1-vs-all protocols, we have $M(x) \in \{0, 1\}$ and, thus, $\text{CaCE} \in [0, 1]$. A value close to zero indicates that the concept, in isolation, has no causal effect on the outcome of the classification, while a value close to one indicates that the presence/absence of the concept, by itself, can fully control the outcome of the classifier. We discuss the metric in more detail in Section A.2.

3.6. Stage 5: Exploring the explanation space

The best-case scenario after Stage 4 is having a single explanation with a very high CaCE, indicating it fully captures the decision rule of the model. However, we cannot expect this ideal immediate outcome for complex classifiers that rely on an intricate combination of features.

Fortunately, the framework of Stage 4 allows for exploring the space of explanations by combining and varying them, automatically or with human guidance, to gain a deeper understanding of the model. The combined explanations are then re-evaluated using Stage 4 to measure their causal impact on the model’s output. Such refinement,

shown on the right side of Figure 2, allows users to improve their understanding of the model’s decision.

4. Experiments

We evaluate GIFT on three use cases of increasing complexity. In Section 4.1, we test GIFT’s ability to uncover classification rules in a controlled setting with the CLEVR dataset [45]. In Section 4.2, we showcase how an exploration guided by GIFT finds detailed explanations for a classifier trained on CelebA [51]. Finally, in Section 4.3, we use GIFT to reveal biases in a model trained on BDD-OIA [85], a dataset of complex driving scenes. In Section 4.4, we present evidences on the importance of the stages.

4.1. Uncovering classification rules on CLEVR

Here, the goal is for GIFT to explain the decisions of a model M , expressing the rules of M in natural language. The setting is challenging, as we do not provide any prior knowledge on M to GIFT, not even the possible class meaning.

Data and target classifiers. We use the CLEVR dataset [45], which presents synthetic but photorealistic arrangements of objects with various shapes, colors, and textures on a neutral background. We train various target classifiers on binary tasks to recognize a specific visual rule such as ‘cyan object present’ or ‘yellow rubber object present’. CLEVR images hide complex compositional potential behind their minimalist appearance, with diverse colors, textures, and shapes. Uncovering the underlying rule in each classifier from local examples is challenging, even for humans. We include both ViT-Small-Patch16-224 [15] and ResNet-34 [35] architectures. Our evaluation comprises 12 unique combinations of visual rule \times architecture.

Instantiation of GIFT. Counterfactual explanation generation (Stage 1) uses OCTET [88], based on a BlobGAN [16] generative model that we trained on CLEVR. Change-captioning (Stage 2) employs CLIP4IDC [32], trained on the CLEVR-Change dataset [57]. The LLM of Stage 3 is

Rule	Arch.	GIFT	Abl.	CaCE
Cyan object	ResNet	✓	×	62
Purple object	ResNet	✓	✓	71
Metal object	ResNet	✓	✓	24
Rubber object	ResNet	✓	×	30
Red metal object	ResNet	×	×	N/A
Yellow rubber object	ResNet	✓	×	67
<hr/>				
Cyan object	ViT	✓	×	63
Purple object	ViT	✓	✓	70
Metal object	ViT	✓	✓	37
Rubber object	ViT	✓	×	31
Red metal object	ViT	✓	×	71
Yellow rubber object	ViT	✓	×	72

Table 1. **Classification rule reverse engineering on CLEVR.** Success criterion is to have the hidden true rule on top after ranking them by the CaCE causal effect metric (Eq. 3) after a single pass of Stages 1–4. GIFT succeeds for all but one case. An ablation (Abl.) with descriptive captions instead of change captions misses most rules (Sec. 4.4). A qualitative analysis of the failure case ‘Red metal object / ResNet’ appears in Sec. 2. CaCE in %.

ChatGPT4 [56]. Interventions (Stage 4) use a Stable Diffusion model [64] adapted to CLEVR for targeted addition and removal of objects [12]. The VQA model (Stage 4) is MiniCPM [84].

Main results. Table 1 reports the trials of GIFT uncovering the hidden visual rule underlying the target classifiers after a *single round* of Stages 1–4. The true visual rule was uncovered in all but one of the 12 cases.

Explanation verification (Stage 4) turns out to be critical to uncover the true rule. Global explanation extraction (Stage 3) finds 2 to 6 rules for each target classifier. Without Stage 4 and ranking by CaCE (Section 3.5) the user has no guidance to distinguish them. We consider the trial successful when the true rule appears on top after Stage 4 and ranking by CaCE.

The failure case of ‘Red metal object’ on ResNet-34 is interesting, for it showcases the interest in combining explanations (Stage 5). We provide a detailed qualitative analysis of this case in Figure 2, which, besides overviewing the whole of GIFT, shows actual experimental data for that trial. (Stage 1:) Counterfactual image generation flips the model’s decision by modifying objects’ presence, location, or appearance. (Stage 2:) Because each counterfactual pair provides a very local and ambiguous explanation, each change caption extracted has weak evidence. There is also some linguistic variation. (Stage 3:) The summarization has to filter out the noise and recover robust trends in the whole sample of captions. However, in this case, it can only recover two partial rules, ‘Red object’ and ‘Metal object’, which (Stage 4) verification tags with a CaCE of 43%

Explanations associated to the class ‘Old’	DI	CaCE
<i>after Stage 3</i>		
Receding Hairline	29.9	6.5
Neck Wrinkles	28.1	3.0
Wrinkles on Forehead	26.4	8.5
Wrinkles around Eyes	20.7	9.0
Glasses	16.5	10.5
Drooping Eyelids	15.4	5.5
Gray Hair	12.3	4.5
...
Pale Skin	0.8	
Detailed Background	0.2	
<hr/>		
<i>after Stage 5</i>		
Gray Hair + Wrinkles around Eyes	39.1	7.8
Hairline + Wrinkles on Forehead	47.8	8.2
Glasses + Wrinkles around Eyes	60.4	21.7
Glasses + Wrinkles on Forehead	59.6	24.1
Glasses + Hairline	61.4	24.6
Glasses + Wrinkles on Forehead + Hairline	78.2	26.0
Glasses + Wrinkles on Forehead + Eyes	65.6	26.8

Table 2. **Output of GIFT on the CelebA ‘Old’ classifier.** The full table is given in Appendix E. DI and CaCE in %.

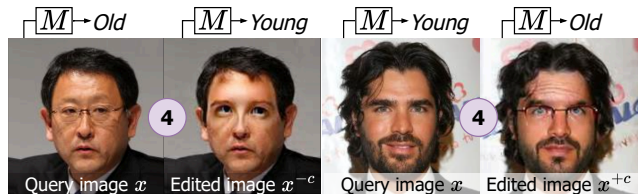


Figure 4. **Samples from the intervention study on the CelebA-‘Old’ classifier.** The combined concepts under scrutiny are: ‘Glasses’, ‘Wrinkles on Forehead’, ‘Wrinkles around Eyes’. Each pair has the query image on the left and the edition on the right.

and 12%, respectively. (Stage 5:) We try combinations of those partial rules and find the true rule ‘Red Metal object’ (CaCE=62%). Both after Stage 3 and Stage 5, verification plays a crucial role in ranking the rules.

4.2. Exploring detailed explanations on CelebA

Here, we use the guidance of GIFT to explore detailed, fine-grained explanations on CelebA [51], a dataset of human faces. CelebA presents additional challenges compared to CLEVR: its data presents all the noise and variability of real life. In addition, subtle changes in facial attributes and expressions may have considerable semantic importance.

Target classifier. The target model M is a DenseNet121 [39] trained to classify face images as either ‘old’ or ‘young’, following [40, 42].

Instantiation of GIFT. Counterfactual generation (Stage

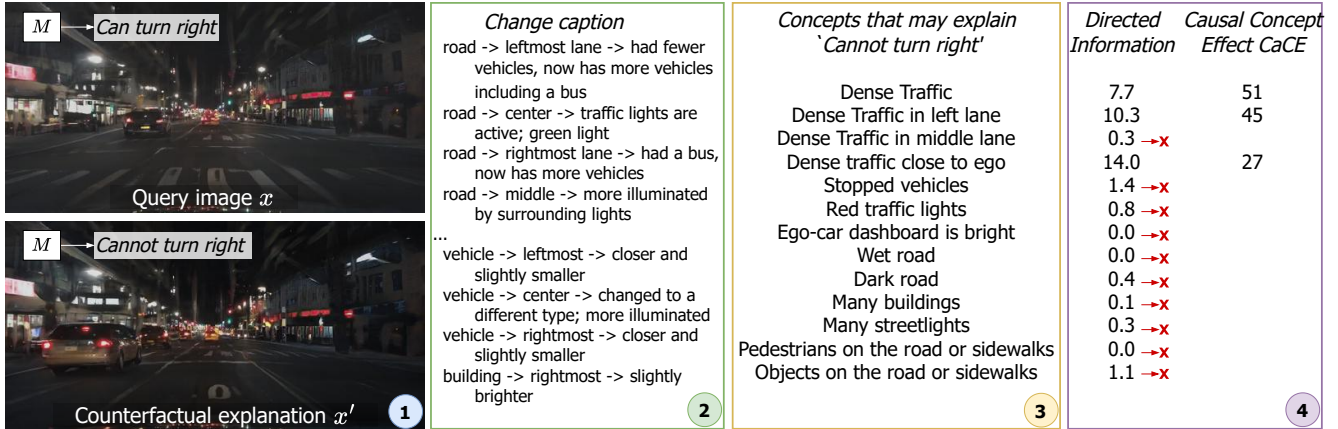


Figure 5. **GIFT output for the biased classifier on BDD-OIA [83]**. The model M classifying images into ‘Can/Cannot turn right’ is intentionally biased for vehicles in the left lane to yield the ‘Cannot turn right’ output. We illustrate the output of Stages 1 and 2 for a single randomly selected input and the global output of Stages 3 and 4.

1) uses the diffusion-based model ACE [42]. Change captioning (Stage 2) employs a Pixtral-12B [3] VLM with a one-shot in-prompt annotated sample as guidance. The concept identification (Stage 3) is performed zero-shot by Qwen 2.5 72B Instruct Quantized on 8-bits [71]. Interventions (Stage 4) use a combination of an image-conditioned version of Stable Diffusion 3 [17] and an in-painting version of Stable Diffusion 2 [64] relying on masks obtained with Florence-2 [82] for targeted editions.

Main results. Table 2 shows a subset of explanatory concepts proposed by GIFT. We note that it includes reasonable attributes, such as ‘wrinkles on the forehead’ and ‘receding hairline’, and more unexpected ones, like a ‘detailed background’. Directed information (DI) scores provide an initial filter to remove explanations whose concepts have no significant relationship to the classifier’s output, allowing us to focus on more promising hypotheses. From that refined set, we conduct intervention studies to measure causal effects. Overall, concepts derived from Stage 3 have low CaCE, meaning that intervening on one attribute alone usually does not change the classifier’s decision. That is a positive indicator for the target classifier, showing that it is relatively robust and not overly reliant on any single attribute to make its decision. However, GIFT finds that adding glasses to individuals classified as ‘young’ or removing them from ‘old’ classifications changes the model’s decision in $\sim 10\%$ of cases. That likely reflects a dataset bias, as ‘has glasses’ correlates with the ‘old’ label in the training data at a rate higher than 20% [73].

As described in Section 3.6, we further explore the explanations by combining and reevaluating them (Table 2, rows ‘after Stage 5’). Some explanations that, individually, have low CaCE yield a much higher CaCE (up to $\sim 26.8\%$) after combination, indicating an increased understanding of

the classifier. Figure 4 illustrates the targeted intervention for the combined attributes ‘Glasses’, ‘Wrinkles on Forehead’, and ‘Wrinkles around Eyes’, which is sufficient to flip the model’s decision in the two query images while leaving the rest of the face mostly unchanged.

4.3. Discovering classifier bias on BDD-OIA

Here, the task is to identify biases in a classifier, i.e., finding among the rules that govern the classifier those that are spurious, incorrect, or undesirable.

Data. We employ BDD-OIA [83], a dataset of front-cam driving scenes in complex urban environments, annotated for admissible actions for the car (turn left, go ahead, turn right, stop/decelerate).

Target classifier. We use a binary classifier for the ‘turn right’ action given in OCTET [88]. They introduced an intentional bias in the training set, systematically assigning images with vehicles on the *left* side to the ‘cannot turn right’ class, in addition to images that would normally belong there. The setup aims to test whether GIFT can uncover this known bias in the target classifier decision.

Instantiation of GIFT. The instantiation of GIFT follows the one of Section 4.2, except for the counterfactual generator, which is OCTET [88] with a BlobGAN [16] trained on BDD100k [83].

Results. Figure 5 shows results for each stage of GIFT, with (1) one sample pair of counterfactual images (of the many generated), (2) the change-caption extracted for it, (3) the relevant concepts the summarizer obtained over many change captions, and (4) the correlation (DI) and causal (CaCE) metrics computed for verification.

In the sample shown in the figure, the counterfactual image presents several changes, including the appearance of a vehicle in the left lane. Due to the complexity of the scenes,

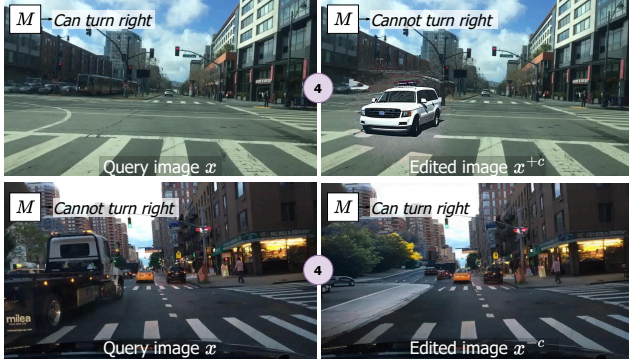


Figure 6. **Image intervention for the ‘Dense Traffic in Left Lane’ explanation.** The model is biased for vehicles in the left lanes to yield the ‘Cannot turn right’ output. Left: query images; Right: images x^{+c} and x^{-c} with the added and removed concept.

individual change captions in this dataset tend to be long and noisy. Again, Stage 3 is critical to condense a large collection of weak signals into a small list of strong, meaningful hypotheses, which, in Stage 4, we can pre-filter with the correlation metric (DI) and then rank by performing the edit interventions and measuring the causal metric (CaCE).

We finish with three strong explanations for being unable to turn right: ‘dense traffic’, ‘dense traffic in left-lane’ (the bias!), and ‘dense traffic close to ego-vehicle’, with, respectively, CaCE of 51, 45, and 27%. While the first and third explanations seem reasonable, the biased explanation uncovered by GIFT should immediately call the attention of anyone evaluating the model.

Figure 6 illustrates some interventions used to confirm those dense-traffic rules, with the addition and removal of vehicles in the left lane in the image.

4.4. Evidence on the importance of the stages

Here, we collect evidence from further experiments, qualitative analyses, and existing literature showcasing the individual importance of each GIFT stage.

Ablation of Stage 2 Here, instead of extracting *change* captions for each counterfactual pair, we extract simple captions for each image in the pair, *independently*. We group the descriptions for each class and ask the LLM (Stage 3), as usual, to find rules governing the classifier’s decision. In the case of CLEVR, the success rate drops from 11/12 to 4/12, as shown in Table 1. The same ablation (change captions → independent description captions) on BDD-OIA bias discovery results in failure to propose the explanation for the bias. Details are in the Appendix D and Appendix F.

Ablation of Stages 1 and 2 on BDD-OIA bias discovery. Previous works show that relying only on LLM-generated hypotheses [1, 13, 30, 59]) or human-proposed hypotheses [88] without counterfactual guidance fails to raise the left-

lane-vehicle bias. More details in Appendix F.

Keeping only Stage 1 for BDD-OIA bias discovery. Using only counterfactual images is the object of OCTET’s user study [88], where participants could inspect several counterfactual explanations. Still, 35% of this group missed the left-lane-vehicle bias, showcasing the interest of Stages 2–4 that translate the evidence into explicitly interpretable natural language.

Stage 3 adaptability to the captions’ information. We evaluate the impact of the number of counterfactual change captions given to Stage 3 on both the CLEVR experiment (Section 4.1) and the BDD-OIA experiment (Section 4.3). In CLEVR, as few as three image pairs provide enough signal for effective summarization, while in BDD-OIA, ~ 20 pairs are needed. That showcases how Stage 2 does not suffice alone: one single change caption from one single image-pair has simply too little information. Stage 3 crucial role is extracting the combined evidence from all (many or few, depending on the problem’s complexity) change captions and proposing promising global explanations.

Stage 4 importance for selecting the best rules. Stage 4 is critical to select and rank the hypotheses after Stage 3. As mentioned in Section 4.1, each trial on CLEVR raised 2 to 6 viable explanations, which Stage 4 then correctly ranked 11 out of 12 times (Table 1). In Section 4.2, we find dozens of candidate concepts, which Stage 4 reduces to a handful of promising ones (Table 2). In Section 4.3, Stage 4 helps again to focus the attention on the most important concepts, revealing the bias (Figure 5, column 4).

Stage 5 interest for obtaining complex rules. In the CLEVR experiments of Section 4.1, we show that the failure case of ‘red metal object’ on ResNet-34 is salvageable with a round of exploration (Figure 2, rightmost column). In the CelebA experiments of Section 4.2, we explore concept combinations to find explanations with much stronger causal effect (Table 2).

5. Conclusion

GIFT offers a grounded approach for generating global explanations of deep vision models by systematically building from local insights. Starting with instance-level counterfactual explanations, GIFT translates those findings to natural language and aggregates them to identify recurring patterns, allowing global explanations to emerge. Those explanations are then doubly checked, with VQA for high correlation and image interventions for causal effect on the model decisions, ensuring that identified patterns are faithful to the model’s decision-making. GIFT is adaptable to be applicable across various use cases. We hope our proposed framework will motivate further research in zero-shot image change captioning with VLMs, given the exciting new application we open for those models.

Acknowledgments

This work was partially supported by the ANR MultiTrans project (ANR-21-CE23-0032).

References

- [1] Abubakar Abid, Mert Yükekönül, and James Zou. Meaningfully debugging model mistakes using conceptual counterfactual explanations. In *ICML, 2022*. 3, 8
- [2] Julius Adebayo, Justin Gilmer, Michael Muelly, Ian J. Goodfellow, Moritz Hardt, and Been Kim. Sanity checks for saliency maps. In *NeurIPS, 2018*. 2
- [3] Pravesh Agrawal, Szymon Antoniak, Emma Bou Hanna, Devendra Chaplot, Jessica Chudnovsky, Saurabh Garg, Theophile Gervet, Soham Ghosh, Amélie Héliou, Paul Jacob, et al. Pixtral 12b. *arXiv preprint arXiv:2410.07073, 2024*. 7, 20
- [4] Jean-Baptiste Alayrac, Jeff Donahue, Pauline Luc, Antoine Miech, Iain Barr, Yana Hasson, Karel Lenc, Arthur Mensch, Katherine Millican, Malcolm Reynolds, Roman Ring, Eliza Rutherford, Serkan Cabi, Tengda Han, Zhitao Gong, Sina Samangooei, Marianne Monteiro, Jacob L. Menick, Sebastian Borgeaud, Andy Brock, Aida Nematzadeh, Sahand Sharifzadeh, Mikolaj Binkowski, Ricardo Barreira, Oriol Vinyals, Andrew Zisserman, and Karén Simonyan. Flamingo: a visual language model for few-shot learning. In *NeurIPS, 2022*. 4
- [5] Maximilian Augustin, Valentyn Boreiko, Francesco Croce, and Matthias Hein. Diffusion visual counterfactual explanations. In *NeurIPS, 2022*. 2
- [6] David Bau, Bolei Zhou, Aditya Khosla, Aude Oliva, and Antonio Torralba. Network dissection: Quantifying interpretability of deep visual representations. In *CVPR, 2017*. 2
- [7] Hedi Ben-Younes, Éloi Zablocki, Patrick Pérez, and Matthieu Cord. Driving behavior explanation with multi-level fusion. *Pattern Recognit.*, 2022. 1, 2
- [8] Mariusz Bojarski, Anna Choromanska, Krzysztof Choromanski, Bernhard Firner, Larry J Ackel, Urs Muller, Phil Yeres, and Karol Zieba. Visualbackprop: Efficient visualization of cnns for autonomous driving. In *ICRA, 2018*. 1, 2
- [9] Judy Borowski, Roland Simon Zimmermann, Judith Schepers, Robert Geirhos, Thomas S. A. Wallis, Matthias Bethge, and Wieland Brendel. Exemplary natural images explain CNN activations better than state-of-the-art feature visualization. In *ICLR, 2021*. 2
- [10] Tim Brooks, Aleksander Holynski, and Alexei A. Efros. Instructpix2pix: Learning to follow image editing instructions. In *CVPR, 2023*. 23
- [11] Chaofan Chen, Oscar Li, Daniel Tao, Alina Barnett, Cynthia Rudin, and Jonathan Su. This looks like that: Deep learning for interpretable image recognition. In *NeurIPS, 2019*. 2
- [12] Jaemin Cho, Linjie Li, Zhengyuan Yang, Zhe Gan, Lijuan Wang, and Mohit Bansal. Diagnostic benchmark and iterative inpainting for layout-guided image generation. In *CVPR Workshop, 2024*. 6
- [13] Gabriela Csurka, Tyler L Hayes, Diane Larlus, and Riccardo Volpi. What could go wrong? discovering and describing failure modes in computer vision. *arXiv preprint arXiv:2408.04471, 2024*. 3, 8
- [14] Sanjoy Dasgupta, Nave Frost, and Michal Moshkovitz. Framework for evaluating faithfulness of local explanations. In *ICML, 2022*. 1
- [15] Alexey Dosovitskiy, Lucas Beyer, Alexander Kolesnikov, Dirk Weissenborn, Xiaohua Zhai, Thomas Unterthiner, Mostafa Dehghani, Matthias Minderer, Georg Heigold, Sylvain Gelly, Jakob Uszkoreit, and Neil Houlsby. An image is worth 16x16 words: Transformers for image recognition at scale. In *ICLR, 2021*. 5
- [16] Dave Epstein, Taesung Park, Richard Zhang, Eli Shechtman, and Alexei A. Efros. Blobgan: Spatially disentangled scene representations. In *ECCV, 2022*. 5, 7, 15, 21, 23
- [17] Patrick Esser, Sumith Kulal, Andreas Blattmann, Rahim Entezari, Jonas Müller, Harry Saini, Yam Levi, Dominik Lorenz, Axel Sauer, Frederic Boesel, Dustin Podell, Tim Dockhorn, Zion English, and Robin Rombach. Scaling rectified flow transformers for high-resolution image synthesis. In *ICML, 2024*. 7, 16, 20, 23
- [18] Sabri Eyuboglu, Maya Varma, Khaled Kamal Saab, Jean-Benoit Delbrouck, Christopher Lee-Messer, Jared Dunmon, James Zou, and Christopher Ré. Domino: Discovering systematic errors with cross-modal embeddings. In *ICLR, 2022*. 3
- [19] Thomas Fel, Rémi Cadène, Mathieu Chalvidal, Matthieu Cord, David Vigouroux, and Thomas Serre. Look at the variance! efficient black-box explanations with sobol-based sensitivity analysis. In *NeurIPS, 2021*. 1, 2
- [20] Thomas Fel, Thibaut Boissin, Victor Boutin, Agustin Picard, Paul Novello, Julien Colin, Drew Linsley, Tom Rousseau, Rémi Cadène, Lore Goetschalckx, Laurent Gardes, and Thomas Serre. Unlocking feature visualization for deep network with magnitude constrained optimization. In *NeurIPS, 2023*. 1, 3
- [21] Thomas Fel, Victor Boutin, Louis Béthune, Rémi Cadène, Mazda Moayeri, Léo Andéol, Mathieu Chalvidal, and Thomas Serre. A holistic approach to unifying automatic concept extraction and concept importance estimation. In *NeurIPS, 2023*. 1, 2
- [22] Thomas Fel, Agustin Martin Picard, Louis Béthune, Thibaut Boissin, David Vigouroux, Julien Colin, Rémi Cadène, and Thomas Serre. CRAFT: concept recursive activation factorization for explainability. In *CVPR, 2023*. 1, 2, 3
- [23] Ruth C. Fong and Andrea Vedaldi. Interpretable explanations of black boxes by meaningful perturbation. In *ICCV, 2017*. 1, 2
- [24] Timo Freiesleben. Counterfactual explanations & adversarial examples - common grounds, essential differences, and potential transfers. *CoRR*, abs/2009.05487, 2020. 3
- [25] Nicholas Frosst and Geoffrey E. Hinton. Distilling a neural network into a soft decision tree. In *Workshop on Comprehensibility and Explanation in AI and ML @ AI*IA 2017, 2017*. 2
- [26] Robert G Gallager. *Information theory and reliable communication*. Springer, 1968. 4

- [27] Yossi Gandelsman, Alexei A. Efros, and Jacob Steinhardt. Interpreting the second-order effects of neurons in CLIP. *CoRR*, abs/2406.04341, 2024. 2
- [28] Amirata Ghorbani, James Wexler, James Y. Zou, and Been Kim. Towards automatic concept-based explanations. In *NeurIPS*, 2019. 2, 3
- [29] Leilani H. Gilpin, David Bau, Ben Z. Yuan, Ayesha Bajwa, Michael A. Specter, and Lalana Kagal. Explaining explanations: An overview of interpretability of machine learning. In *DSAA*, 2018. 1
- [30] Yash Goyal, Uri Shalit, and Been Kim. Explaining classifiers with causal concept effect (cace). *CoRR*, abs/1907.07165, 2019. 2, 4, 5, 8, 14
- [31] Yash Goyal, Ziyang Wu, Jan Ernst, Dhruv Batra, Devi Parikh, and Stefan Lee. Counterfactual visual explanations. In *ICML*, 2019. 2
- [32] Zixin Guo, Tzu-Jui Julius Wang, and Jorma Laaksonen. CLIP4IDC: CLIP for image difference captioning. In *AAACL/JCNLP*, 2022. 4, 5, 16
- [33] Tanmay Gupta and Aniruddha Kembhavi. Visual programming: Compositional visual reasoning without training. In *CVPR*, 2023. 23
- [34] Michael Harradon, Jeff Druce, and Brian E. Ruttenberg. Causal learning and explanation of deep neural networks via autoencoded activations. *CoRR*, abs/1802.00541, 2018. 2
- [35] Kaiming He, Xiangyu Zhang, Shaoqing Ren, and Jian Sun. Deep residual learning for image recognition. In *CVPR*, 2016. 5
- [36] Lisa Anne Hendricks, Zeynep Akata, Marcus Rohrbach, Jeff Donahue, Bernt Schiele, and Trevor Darrell. Generating visual explanations. In *ECCV*, 2016. 1, 2
- [37] Lisa Anne Hendricks, Ronghang Hu, Trevor Darrell, and Zeynep Akata. Grounding visual explanations. In *ECCV*, 2018. 2
- [38] Mehrdad Hosseinzadeh and Yang Wang. Image change captioning by learning from an auxiliary task. In *CVPR*, 2021. 4
- [39] Gao Huang, Zhuang Liu, Laurens van der Maaten, and Kilian Q. Weinberger. Densely connected convolutional networks. In *CVPR*, 2017. 6, 20
- [40] Paul Jacob, Éloi Zablocki, Hédi Ben-Younes, Mickaël Chen, Patrick Pérez, and Matthieu Cord. STEEX: steering counterfactual explanations with semantics. In *ECCV*, 2022. 1, 2, 6, 20, 23
- [41] Guillaume Jeanneret, Loïc Simon, and Frédéric Jurie. Diffusion models for counterfactual explanations. In *ACCV*, 2022. 2
- [42] Guillaume Jeanneret, Loïc Simon, and Frédéric Jurie. Adversarial counterfactual visual explanations. In *CVPR*, 2023. 1, 2, 3, 6, 7, 20, 21, 23
- [43] Guillaume Jeanneret, Loïc Simon, and Frédéric Jurie. Text-to-image models for counterfactual explanations: a black-box approach. In *WACV*, 2024. 1
- [44] Albert Q. Jiang, Alexandre Sablayrolles, Arthur Mensch, Chris Bamford, Devendra Singh Chaplot, Diego de Las Casas, Florian Bressand, Gianna Lengyel, Guillaume Lample, Lucile Saulnier, Léo Renard Lavaud, Marie-Anne Lachaux, Pierre Stock, Teven Le Scao, Thibaut Lavril, Thomas Wang, Timothée Lacroix, and William El Sayed. Mistral 7b. *CoRR*, abs/2310.06825, 2023. 2
- [45] Justin Johnson, Bharath Hariharan, Laurens van der Maaten, Li Fei-Fei, C. Lawrence Zitnick, and Ross B. Girshick. CLEVR: A diagnostic dataset for compositional language and elementary visual reasoning. In *CVPR*, 2017. 2, 5
- [46] Vidhya Kamakshi, Uday Gupta, and Narayanan C. Krishnan. PACE: posthoc architecture-agnostic concept extractor for explaining cnns. In *IJCNN*. IEEE, 2021. 1, 2
- [47] Saeed Khorram and Fuxin Li. Cycle-consistent counterfactuals by latent transformations. In *CVPR*, 2022. 2
- [48] Been Kim, Martin Wattenberg, Justin Gilmer, Carrie J. Cai, James Wexler, Fernanda B. Viégas, and Rory Sayres. Interpretability beyond feature attribution: Quantitative testing with concept activation vectors (TCAV). In *ICML*, 2018. 1, 2
- [49] Ashish Kumar, Karan Sehgal, Prerna Garg, Vidhya Kamakshi, and Narayanan Chatapuram Krishnan. MACE: model agnostic concept extractor for explaining image classification networks. *IEEE Trans. Artif. Intell.*, 2(6):574–583, 2021. 1, 2
- [50] Jae Hee Lee, Sergio Lanza, and Stefan Wernter. From neural activations to concepts: A survey on explaining concepts in neural networks. *CoRR*, abs/2310.11884, 2023. 2
- [51] Ziwei Liu, Ping Luo, Xiaogang Wang, and Xiaoou Tang. Deep learning face attributes in the wild. In *ICCV*, 2015. 2, 5, 6
- [52] Scott M. Lundberg and Su-In Lee. A unified approach to interpreting model predictions. In *NeurIPS*, 2017. 2
- [53] Zixian Ma, Jerry Hong, Mustafa Omer Gul, Mona Gandhi, Irena Gao, and Ranjay Krishna. CREPE: can vision-language foundation models reason compositionally? In *CVPR*, 2023. 23
- [54] Thomas Mesnard, Cassidy Hardin, Robert Dadashi, Surya Bhupatiraju, Shreya Pathak, Laurent Sifre, Morgane Rivière, Mihir Sanjay Kale, Juliette Love, Pouya Tafti, Léonard Hussenot, Aakanksha Chowdhery, Adam Roberts, Aditya Barua, Alex Botev, Alex Castro-Ros, Ambrose Slone, Amélie Héliou, Andrea Tacchetti, Anna Bulanova, Antonia Paterson, Beth Tsai, Bobak Shahriari, Charline Le Lan, Christopher A. Choquette-Choo, Clément Crepy, Daniel Cer, Daphne Ippolito, David Reid, Elena Buchatskaya, Eric Ni, Eric Noland, Geng Yan, George Tucker, George-Cristian Muraru, Grigory Rozhdestvenskiy, Henryk Michalewski, Ian Tenney, Ivan Grishchenko, Jacob Austin, James Keeling, Jane Labanowski, Jean-Baptiste Lespiau, Jeff Stanway, Jenny Brennan, Jeremy Chen, Johan Ferret, Justin Chiu, and et al. Gemma: Open models based on gemini research and technology. *CoRR*, abs/2403.08295, 2024. 2
- [55] Daniel Omeiza, Helena Webb, Marina Jirotko, and Lars Kunze. Explanations in autonomous driving: A survey. *IEEE Trans. Intell. Transp. Syst.*, 2022. 1
- [56] OpenAI. GPT-4 technical report. *CoRR*, abs/2303.08774, 2023. 6
- [57] Dong Huk Park, Trevor Darrell, and Anna Rohrbach. Robust change captioning. In *ICCV*, 2019. 5, 15, 16

- [58] Judea Pearl. *Causality*. Cambridge university press, 2009. 2, 4
- [59] Viraj Prabhu, Sriram Yenamandra, Prithvijit Chattopadhyay, and Judy Hoffman. LANCE: stress-testing visual models by generating language-guided counterfactual images. In *NeurIPS*, 2023. 1, 3, 8
- [60] Yue Qiu, Yutaka Satoh, Ryota Suzuki, Kenji Iwata, and Hirokatsu Kataoka. 3d-aware scene change captioning from multiview images. *IEEE Robotics Autom. Lett.*, 5(3):4743–4750, 2020. 4
- [61] Arijit Ray, Filip Radenovic, Abhimanyu Dubey, Bryan A. Plummer, Ranjay Krishna, and Kate Saenko. Cola: A benchmark for compositional text-to-image retrieval. In *NeurIPS*, 2023. 23
- [62] Marco Túlio Ribeiro, Sameer Singh, and Carlos Guestrin. "why should I trust you?": Explaining the predictions of any classifier. In *SIGKDD*, 2016. 2
- [63] Pau Rodríguez, Massimo Caccia, Alexandre Lacoste, Lee Zamparo, Issam H. Laradji, Laurent Charlin, and David Vázquez. Beyond trivial counterfactual explanations with diverse valuable explanations. In *ICCV*, 2021. 1, 2
- [64] Robin Rombach, Andreas Blattmann, Dominik Lorenz, Patrick Esser, and Björn Ommer. High-resolution image synthesis with latent diffusion models. In *CVPR*, 2022. 6, 7, 20
- [65] Cynthia Rudin. Stop explaining black box machine learning models for high stakes decisions and use interpretable models instead. *Nat. Mach. Intell.*, 1(5):206–215, 2019. 1
- [66] Ramprasaath R. Selvaraju, Michael Cogswell, Abhishek Das, Ramakrishna Vedantam, Devi Parikh, and Dhruv Batra. Grad-cam: Visual explanations from deep networks via gradient-based localization. In *ICCV*, 2017. 1, 2
- [67] Bartłomiej Sobieski and Przemysław Biecek. Global counterfactual directions. In *ECCV*, 2024. 2
- [68] Wolfgang Stammer, Patrick Schramowski, and Kristian Kersting. Right for the right concept: Revising neuro-symbolic concepts by interacting with their explanations. In *CVPR*, 2021. 15
- [69] Mukund Sundararajan, Ankur Taly, and Qiqi Yan. Axiomatic attribution for deep networks. In *ICML*, 2017. 1, 2
- [70] Christian Szegedy, Wojciech Zaremba, Ilya Sutskever, Joan Bruna, Dumitru Erhan, Ian J. Goodfellow, and Rob Fergus. Intriguing properties of neural networks. In *ICLR*, 2014. 3
- [71] Qwen Team. Qwen2.5: A party of foundation models, 2024. 7, 20
- [72] Erico Tjoa and Cuntai Guan. A survey on explainable artificial intelligence (XAI): towards medical XAI. *CoRR*, abs/1907.07374, 2019. 1
- [73] Robert Torfason, Eirikur Agustsson, Rasmus Rothe, and Radu Timofte. From face images and attributes to attributes. In *ACCV*, 2016. 7
- [74] Simon Vandenhende, Dhruv Kumar Mahajan, Filip Radenović, and Deepti Ghadiyaram. Making heads or tails: Towards semantically consistent visual counterfactuals. In *ECCV*, 2022. 2
- [75] Sandra Wachter, Brent Mittelstadt, and Chris Russell. Counterfactual explanations without opening the black box: Automated decisions and the gdpr. *Harvard Journal of Law & Technology*, 2017. 1, 2
- [76] Jörg Wagner, Jan Mathias Köhler, Tobias Gindele, Leon Hetzel, Jakob Thaddäus Wiedemer, and Sven Behnke. Interpretable and fine-grained visual explanations for convolutional neural networks. In *CVPR*, 2019. 1, 2
- [77] Pei Wang and Nuno Vasconcelos. SCOUT: self-aware discriminant counterfactual explanations. In *CVPR*, 2020. 2
- [78] Yixin Wang and Michael I. Jordan. Desiderata for representation learning: A causal perspective. *CoRR*, abs/2109.03795, 2021. 15
- [79] Yinong Oliver Wang, Eileen Li, Jinqi Luo, Zhaoning Wang, and Fernando De la Torre. Unsupervised model diagnosis. *arXiv preprint arXiv:2410.06243*, 2024. 3
- [80] Jason Wei, Xuezhi Wang, Dale Schuurmans, Maarten Bosma, Brian Ichter, Fei Xia, Ed H. Chi, Quoc V. Le, and Denny Zhou. Chain-of-thought prompting elicits reasoning in large language models. In *NeurIPS*, 2022. 23
- [81] Olivia Wiles, Isabela Albuquerque, and Sven Gowal. Discovering bugs in vision models using off-the-shelf image generation and captioning. *CoRR*, abs/2208.08831, 2022. 3
- [82] Bin Xiao, Haiping Wu, Weijian Xu, Xiyang Dai, Houdong Hu, Yumao Lu, Michael Zeng, Ce Liu, and Lu Yuan. Florence-2: Advancing a unified representation for a variety of vision tasks. In *CVPR*, 2024. 7, 15, 16, 20, 22
- [83] Yiran Xu, Xiaoyin Yang, Lihang Gong, Hsuan-Chu Lin, Tz-Ying Wu, Yunsheng Li, and Nuno Vasconcelos. Explainable object-induced action decision for autonomous vehicles. In *CVPR*, 2020. 7
- [84] Yuan Yao, Tianyu Yu, Ao Zhang, Chongyi Wang, Junbo Cui, Hongji Zhu, Tianchi Cai, Haoyu Li, Weilin Zhao, Zhihui He, Qianyu Chen, Huarong Zhou, Zhensheng Zou, Haoye Zhang, Shengding Hu, Zhi Zheng, Jie Zhou, Jie Cai, Xu Han, Guoyang Zeng, Dahai Li, Zhiyuan Liu, and Maosong Sun. Minicpm-v: A GPT-4V level MLLM on your phone. *CoRR*, abs/2408.01800, 2024. 6, 16, 20
- [85] Fisher Yu, Haofeng Chen, Xin Wang, Wenqi Xian, Yingying Chen, Fangchen Liu, Vashisht Madhavan, and Trevor Darrell. BDD100K: A diverse driving dataset for heterogeneous multitask learning. In *CVPR*, 2020. 2, 5
- [86] Éloi Zablocki, Hédi Ben-Younes, Patrick Pérez, and Matthieu Cord. Explainability of deep vision-based autonomous driving systems: Review and challenges. *IJCV*, 2022. 1
- [87] Matthew D. Zeiler and Rob Fergus. Visualizing and understanding convolutional networks. In *ECCV*, 2014. 1, 2
- [88] Mehdi Zemni, Mickaël Chen, Éloi Zablocki, Hédi Ben-Younes, Patrick Pérez, and Matthieu Cord. OCTET: object-aware counterfactual explanations. In *CVPR*, 2023. 1, 2, 3, 5, 7, 8, 15, 21, 22, 23
- [89] Quanshi Zhang, Ruiming Cao, Feng Shi, Ying Nian Wu, and Song-Chun Zhu. Interpreting CNN knowledge via an explanatory graph. In *AAAI*, 2018. 2
- [90] Quanshi Zhang, Ying Nian Wu, and Song-Chun Zhu. Interpretable convolutional neural networks. In *CVPR*, 2018. 1, 2
- [91] Ruihan Zhang, Prashan Madumal, Tim Miller, Krista A. Ehinger, and Benjamin I. P. Rubinstein. Invertible concept-based explanations for CNN models with non-negative concept activation vectors. In *AAAI*, 2021. 1, 2

- [92] Bolei Zhou, Aditya Khosla, Àgata Lapedriza, Aude Oliva, and Antonio Torralba. Object detectors emerge in deep scene cnns. In *ICLR*, 2015. [1](#), [2](#)
- [93] Jan Ruben Zilke, Eneldo Loza Mencía, and Frederik Janssen. Deepred - rule extraction from deep neural networks. In *DS*, 2016. [2](#)

GIFT: A Framework for Global Interpretable Faithful Textual Explanations of Vision Classifiers

Supplementary Material

Contents

1. Introduction	1
2. Related Work	2
3. GIFT Framework	3
3.1. Overview	3
3.2. Stage 1: Faithful visual and local explanations	3
3.3. Stage 2: From visual counterfactuals to text . . .	4
3.4. Stage 3: Candidate global explanations	4
3.5. Stage 4: Hypotheses verification	4
3.6. Stage 5: Exploring the explanation space	5
4. Experiments	5
4.1. Uncovering classification rules on CLEVR	5
4.2. Exploring detailed explanations on CelebA	6
4.3. Discovering classifier bias on BDD-OIA	7
4.4. Evidence on the importance of the stages	8
5. Conclusion	8
A Details on hypotheses verification (stage 4)	13
A.1 Directed information (DI)	13
A.2 Causal Concept Effect (CaCE)	14
B LLM prompts (stage 3) and ablations.	15
C VLM prompts (stage 2)	15
D Experimental Details on CLEVR	15
D.1. CLEVR: a challenging compositional domain	15
D.2 CLEVR Classifiers	15
D.3 GIFT Instantiation	15
D.4 Results	16
E Experimental Details on CelebA	20
E.1. GIFT Instantiation	20
E.2. Results	20
F. Experimental Details on BDD-OIA bias discovery	20
F.1. GIFT Instantiation	20
F.2. Results	21
G Limitations	23

A. Details on hypotheses verification (stage 4)

A.1. Directed information (DI)

We provide detailed steps for computing Directed Information (DI), Equation 1 described in Section 3.5, that evaluates the correlation between concepts c_e and class labels y . DI is computed as:

$$DI(c_e, y) = \frac{I(c_e; y)}{H(c_e)},$$

where $I(c_e; y)$ is the mutual information and $H(c_e)$ is the entropy. Below, we explain each term and outline how they are computed.

Mutual Information $I(c_e; y)$

Mutual information quantifies the amount of information the presence of concept c_e provides about the predicted class label y . It is defined as:

$$I(c_e; y) = \sum_{c_e, y} p(c_e, y) \log \left(\frac{p(c_e, y)}{p(c_e)p(y)} \right),$$

where:

- $p(c_e, y)$ is the joint probability of the concept c_e and class label y ,
- $p(c_e)$ is the marginal probability of c_e ,
- $p(y)$ is the marginal probability of y .

We use the outputs of a Visual Question Answering (VQA) model to estimate $p(c_e, y)$. The VQA model predicts whether the concept c_e is present in an input image x . For a dataset of images \mathcal{X} , we calculate:

$$p(c_e, y) = \frac{1}{|\mathcal{X}|} \sum_{x \in \mathcal{X}} \mathbb{1}[\text{VQA}(x, c_e) = 1 \wedge M(x) = y],$$

where $\mathbb{1}[\cdot]$ is the indicator function, and $|\mathcal{X}|$ the cardinal of the set \mathcal{X} . The marginal $p(c_e)$ and $p(y)$ are derived from the joint probabilities:

$$p(c_e) = \sum_y p(c_e, y), \quad p(y) = \sum_{c_e} p(c_e, y).$$

Entropy of the Concept Presence ($H(c_e)$)

Entropy measures the uncertainty in the presence of concept c_e across the dataset. It is defined as:

$$H(c_e) = - \sum_{c_e} p(c_e) \log p(c_e).$$

We use the marginal probability $p(c_e)$ estimated above.

Each one of the descriptions below (separated by ‘—’) details the changes a pair of images underwent as part of a counterfactual analysis for a machine-learning binary classifier. The described changes caused the classifier to change its prediction either from class 0 to class 1 or from class 1 to class 0. Your task is to consider ALL the descriptions and summarize the main factors leading the classifier to choose class 0 or 1.

- The counterfactual analysis is noisy, and the descriptions may contain irrelevant or contradictory information. Your task is to focus on the most important factors that appear consistently across many instances

- Find testable factors that can be observed and measured in the images (e.g., objects’ presence, appearance, arrangement, etc.)

- Present your factors as a bulleted list

—
From class 0 to class 1:

left car → closer; more visible headlights

ego-car → dashboard → brighter

...

—
From class 0 to class 1:

traffic → leftmost lane → was clear, now a taxi is present

traffic → rightmost lane → was clear, now is occupied by cars

...

Figure 7. **Prompt used for the LLM in Stage 3.** This prompt is utilized across all experimental use cases. The ellipses ‘...’ are placeholders, replaced with the concatenation of all change captions gathered in stage 2. Note that the class labels are not provided; instead, they are represented generically as 0 or 1.

A.2. Causal Concept Effect (CaCE)

We discuss the CaCE metric that we used in Section 3.5. As before, $c_e \in \mathcal{C}$ denotes a concept associated with an explanation $e \in \mathcal{E}$, x represents an image from a set \mathcal{X} of observed images, typically the validation set, and $\tilde{x} = EDIT(x, c_e)$ where EDIT is a stochastic process, implemented with a stable diffusion model in our experiments, aiming to add (resp. remove) concept c_e and generate x^{+c_e} (resp. x^{-c_e}) from x if it is absent from (resp. present in) x . $M(x) \in \{0, 1\}$ is the model decision on input x for our binary classifier M . We have then the Individual Causal Effect (ICE):

$$ICE(x) = \begin{cases} M(x^{+c_e}) - M(x) & \forall x \in \mathcal{X}_{c_e=0} \\ M(x) - M(x^{-c_e}) & \forall x \in \mathcal{X}_{c_e=1}, \end{cases} \quad (4)$$

The Causal Concept Effect (CaCE) defined in [30] averages ICE across all images:

$$CaCE_{\text{original}} = \frac{1}{|\mathcal{X}|} \sum_{x \in \mathcal{X}} ICE(x) \quad (5)$$

$CaCE_{\text{original}} \in [-1, 1]$ with the following implications, for a chosen relevance threshold ϵ :

- if $CaCE_{\text{original}} < -\epsilon$, then the **presence of c_e “entails” class 0** and its absence “entails” class 1
- if $CaCE_{\text{original}} > \epsilon$, then the **presence of c_e “entails” class 1** and its absence “entails” class 0

- if $-\epsilon \leq CaCE_{\text{original}} \leq \epsilon$ then c_e does not impact the classification decision

Note that in Section 3.5, we present a slightly modified version of CaCE, using an absolute value around the global sum:

$$CaCE_{\text{ours}} = \frac{1}{|\mathcal{X}|} \left| \sum_{x \in \mathcal{X}} ICE(x) \right| \quad (6)$$

The main motivation behind the use of this CaCE version is that the two first implications of $CaCE_{\text{original}}$ are merged in $CaCE_{\text{ours}}$, as follows:

- if $CaCE_{\text{ours}} > \epsilon$, then the presence (resp. absence) of c_e consistently changes the class decision in one direction, e.g., $0 \rightarrow 1$, (resp. in the other direction, e.g. $1 \rightarrow 0$)
- if $CaCE_{\text{ours}} \leq \epsilon$ then c_e does not impact the classification decision

The use of $CaCE_{\text{ours}}$ rather than $CaCE_{\text{original}}$ in this work serves several purposes. Merging the two first implications of $CaCE_{\text{original}}$ enables us to be robust to label switching, especially for our experimental use case 1. Indeed, as we are reverse-engineering the underlying classification task, we want to evaluate simultaneously if an identified concept c_e is consistently changing the class decision, regardless of the label naming (whether the class change is $0 \rightarrow 1$ or $1 \rightarrow 0$). Moreover, while the sign of $CaCE_{\text{original}}$ can be used to verify whether the concept is indeed explaining the class 0 or 1, we do not need such granularity, even in our

experimental use cases 2 and 3, as the LLM’s explanations $e \in \mathcal{E}$ are indicating specifically which class we are trying to explain with underlying concept c_e . Using $\text{CaCE}_{\text{ours}}$ thus enables us to use a unified causal metric across our three use cases, normalized to belong to $[0, 1]$.

Other candidate causal metrics. CaCE is not the only causal metric we could have used. Another relevant candidate metric for measuring causality, especially for broader scenarios than ours, going beyond binary classification tasks, would be to use an approximation of the probability of the chosen concept to be both a *necessary cause* and a *sufficient cause* of a specific label $\mathbb{1}_{Y=y}$, as defined in [78].

B. LLM prompts (stage 3) and ablations.

Default LLM prompt for stage 3. We report in Figure 7 the prompt that we used to summarize change captions and make global hypotheses emerge. The prompt is exemplified for the BDD experiments but is identical for CLEVR and CelebA experiments.

LLM prompt (stage 3) for the ablation of stage 2. In the baseline, described in Section 4.4 (‘Ablation of Stage 2’), instead of feeding the LLM with *change captions*, we provide simple captions for all images and counterfactuals. To generate the captions for each image, we use the recent Florence-2 [82], prompted with the ‘More detailed captions’ mode. Then, we feed all the captions, along with the classification yielded by the target model M , to the LLM, with a prompt shown in Figure 14. LLM fails to hypothesize that Class ‘1’ is confounded by the presence of vehicles in the left-lane. This ablation highlights the importance of fine-grained pairwise comparisons between an image and its counterfactual explanation, as provided by stage 2, are crucial for the effectiveness of our method.

LLM prompt (stage 3) for the ablation of stages 1 and 2. In the baseline, described in Section 4.4 (‘Ablation of Stages 1 and 2’), we prompt the LLM of Stage 3 to imagine possible biases that the target classifier may suffer. There are thus no counterfactual explanations generation and the LLM does not depend on any information given by the classifier, except for the class meaning (=labels). We show the prompt and output in Figure 15. As there are no dependencies anymore on the target classifier, the LLM can only imagine generic biases and fails to find the unexpected left-lane bias. As LLM-generated hypotheses fail to raise the left-lane-vehicle bias, it shows the importance of the counterfactual guidance (stages 1 and 2) in the GIFT framework

* Answer: ‘Images of class 1 contain a cyan metallic object.’

C. VLM prompts (stage 2)

We report in Figure 12 and Figure 13 the prompts that we use to prompt Pixtral for image change captioning, for BDD and CelebA experiments respectively. We use a one-shot in-prompt annotated sample as guidance, where we manually describe the differences between an image (randomly selected) and the obtained counterfactual explanation after stage 1. We qualitatively find that this guides the VLM to produce more accurate change captions.

In the case of CLEVR, we use CLIP4IDC which is trained for the image change captioning task on the CLEVR domain, with the annotated CLEVR-Change [57] dataset.

D. Experimental Details on CLEVR

D.1. CLEVR: a challenging compositional domain

Figure 8 presents a challenge to the reader to uncover the underlying visual rule learned by the classifier M . In this example, M has been trained on a specific rule, such as ‘images in class 1 contain a yellow rubber object’ or ‘images in class 0 contain a red object’, similar to the setup described in Section 4.1. By observing the images and the model’s predictions, the reader is invited to deduce the rule. This task highlights the inherent complexity of the CLEVR dataset, where simple appearances mask intricate combinations of colors, textures, and shapes. The solution to the challenge is provided in the footnote at the end of the figure caption.

D.2. CLEVR Classifiers

We use CLEVR-Hans [68] to generate six binary classification datasets with BLENDER. The images are then resized and center-cropped to 128×128 to match the resolution of the BlobGAN generative model. The training and validation sets contain 3,000 and 300 samples, respectively, with balanced labels. We train 12 classifiers (listed in Table 1) with either ViT or ResNet34 backbones on these datasets, selecting the checkpoint with the best validation accuracy from the first three epochs. For all these classifiers, we report near-perfect validation accuracies, ranging from 96.3% to 99.3%.

D.3. GIFT Instantiation

Stage 1. To instantiate GIFT on the CLEVR domain, we first require a method for counterfactual explanation (stage 1). For this, we employ OCTET [88], which produces ‘object-aware’ explanations and is well-suited for the object-centric nature of CLEVR. However, since the official OCTET implementation is not compatible with CLEVR, we reimplemented it for this domain. A key component of this adaptation is BlobGAN [16], a compositional generative model capable of editing, inserting, and removing

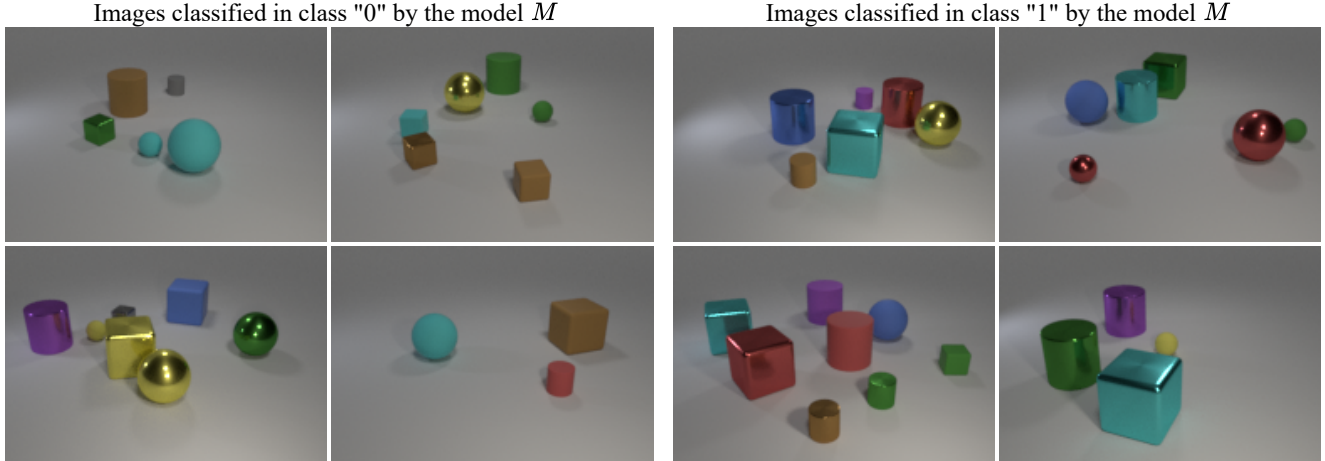


Figure 8. **Can you find the class meaning?** We propose a challenge to the reader. The classifier M has been trained to recognize a specific visual rule, e.g., ‘images in class 1 contain a yellow rubber object’, as with the experiments of Section 4.1. Can you guess what is the rule simply by observing the images and their classification given by the model M ? This challenge illustrates the difficulty of the CLEVR data domain: CLEVR images hide complex compositional potential behind their minimalist appearance, with diverse colors, textures, and shapes. The answer is given in the footnote *.

objects in a differentiable manner. We trained BlobGAN on the original CLEVR dataset. The images were resized and center-cropped to 128×128 resolution. We used $K = 15$ blobs, slightly exceeding the maximum number of objects (10) in a CLEVR scene. The BlobGAN training was conducted for 181 epochs. Notably, we did not need to retrain an image encoder. Instead, we directly sample within BlobGAN’s latent space to generate the original query image. This approach not only produced satisfying results but also circumvented the need for computationally intensive image reconstructions, which are typically required in the first step of OCTET optimization.

Stage 2. For the image change captioning (stage 2), we use CLIP4IDC [32], which is specifically designed for the CLEVR dataset. This model is trained on CLEVR-Change [57], a dataset that includes image pairs and textual *change captions* describing the differences between the images. We note that since the CLEVR-Change dataset does include shape or size changes (e.g., a sphere turning into a cylinder, or a small sphere is now a big sphere), CLIP4IDC is unable to describe such transformations. As a result, we only consider rules that do not rely on shape or size, as counterfactual explanations produced with OCTET would include such changes that CLIP4IDC cannot translate into natural language. In contrast, for the other use-cases with CelebA and BDD-OIA, we do not face this limitation as we use generalist VLMs. However, these models are somewhat noisier since they were not specifically trained for this task.

Stage 4. In stage 4, hypothesis verification was conducted using 200 images: 100 classified as 1 by the model and 100 classified as 0. Importantly, we never accessed the ground-truth labels. For concept verification in stage 4 and the DI computation, we utilized the MiniCPM [84] model. Interventions in stage 4 involved object additions and removals:

- **Object addition:** We identified empty regions in the image by checking if the mean pixel value and standard deviation within a selected area were close to the background color and zero, respectively. This produced a mask that was passed to Stable Diffusion [17] alongside the description of the object to add, e.g., ‘a cyan object’. The model then placed the object in the specified region.
- **Object removal:** We identified the bounding boxes of the objects to remove using Florence-2 [82] in ‘CAPTION_TO_PHRASE.GROUNDING’ mode. Subsequently, Stable Diffusion [17] was used to inpaint these regions with the word ‘background’, effectively removing the objects.

D.4. Results

Qualitative samples after stages 1 and 2. Figure 9 provides qualitative examples from stages 1 and 2, highlighting the outputs of the counterfactual generator (CEX) and the change captioner (CC). The counterfactual explanation optimization depends on three inputs: the original image, the model decision to be flipped, and the model itself (illustrated with blue boxes and arrows). In contrast, the image change captioning stage relies solely on the pair of input images (indicated by the green box). The counterfactual explanations exhibit notable diversity, encompassing changes

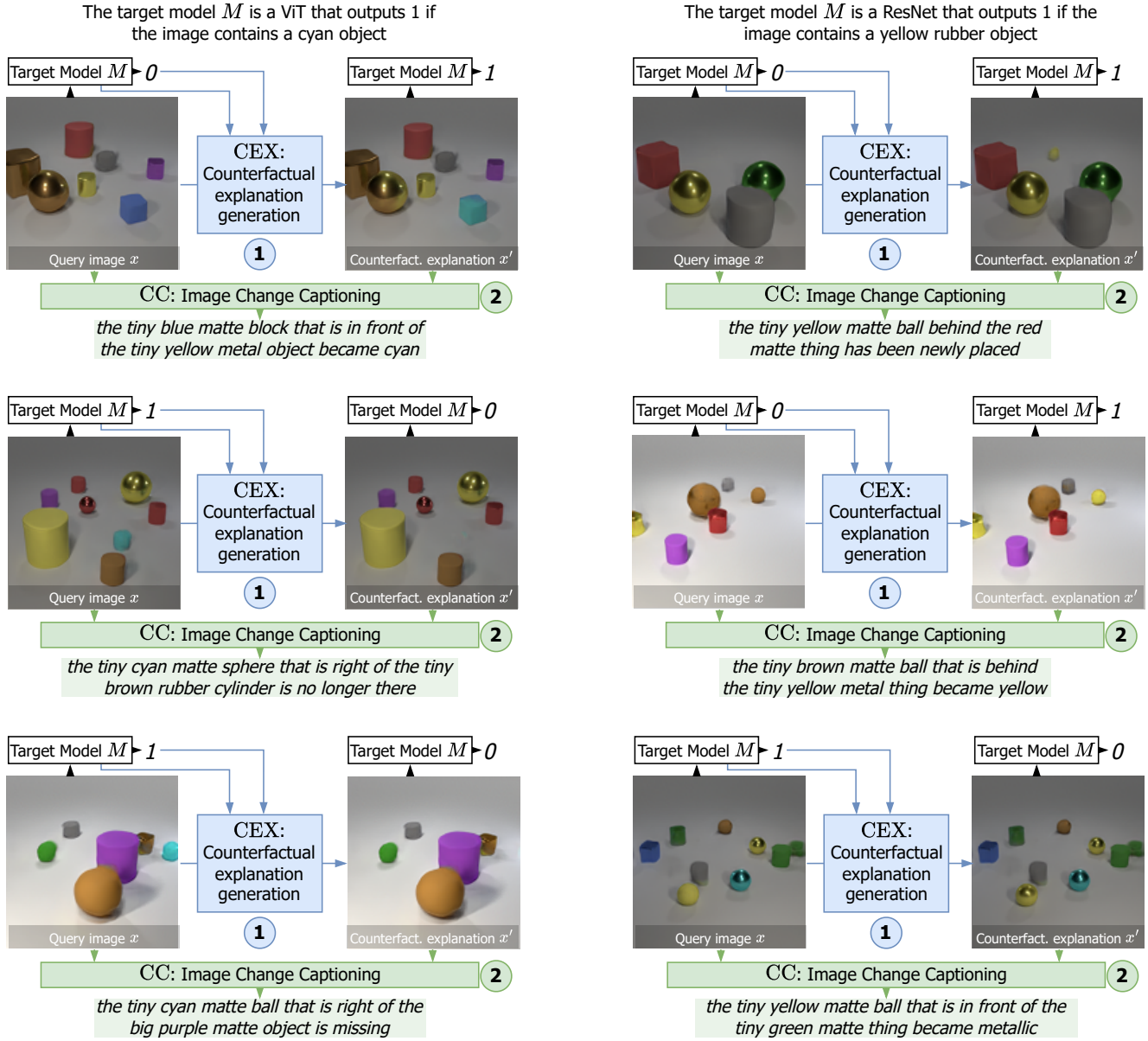


Figure 9. **Visualization of the Stages 1 and 2** for classifiers trained on CLEVR data. CEX generates a counterfactual explanation and CC describes differences in plain text. Examples on the left block are obtained for a model M that outputs ‘1’ if the image contains a cyan object. Examples on the right block are obtained for a model M that outputs ‘1’ if the image contains a yellow rubber object. The counterfactual explanations exhibit notable diversity, encompassing changes in object colors, appearances, disappearances, and textures. Furthermore, the CLIP4IDC model, specifically trained for this task, excels at translating visual changes into natural language descriptions. Its outputs are consistently accurate, with minimal noise and rare errors.

in object colors, appearances, disappearances, and textures. Furthermore, the CLIP4IDC model, specifically trained for this task, excels at translating visual changes into natural language descriptions. Its outputs are consistently accurate, with minimal noise and rare errors.

Complete results. Table 3 summarizes the results of stages 3 and 4 across the 12 classifiers tested on the CLEVR dataset. Notably, in all but one case, the rule that governed the target classifier was correctly proposed by the large language model (LLM) after stage 3. Stage 3 outputs reveal that the LLM generates a small set of hypotheses (between 1 and 5). In certain instances, only a single hypothesis is

Rule	Architecture	Output of Stage 3	Output of Stage 4	
		Explanation: ‘Class 1 contains a...’	DI (%)	CaCE (%)
cyan object	ResNet34	cyan object	96.8	62.2
		cyan metal object	26.0	50.9
		cyan rubber object	31.2	47.6
purple object	ResNet34	purple object	92.9	71.2
metal object	ResNet34	red object	0.2	8.6
		metal object	88.9	24.2
rubber object	ResNet34	rubber object	66.5	29.8
yellow rubber object	ResNet34	yellow rubber object	44.3	67.2
		small yellow rubber sphere	14.1	57.6
		yellow object	31.0	38.4
red metal object	ResNet34	red object	46.8	42.9
		metal object	3.6	11.6
		<i>red metal object</i>	65.5	61.6
cyan object	ViT	cyan object	92.9	63.1
		cyan sphere	24.4	50.5
		cyan cube	28.0	42.4
purple object	ViT	purple sphere	17.2	52.5
		purple cylinder	29.6	53.0
		purple object	92.9	70.2
metal object	ViT	metal object	83.4	37.4
		rubber object	16.3	5.6
		red metal object	14.7	36.4
		yellow metal object	14.7	34.8
rubber object	ViT	green metal object	10.8	29.3
		rubber object	62.0	30.8
		blue object	0.0	8.6
yellow rubber object	ViT	cyan object	0.6	7.6
		yellow rubber object	51.2	71.7
red metal object	ViT	yellow object	42.4	49.0
		metal object	0.3	12.6
		red metal object	63.2	70.7
		red object	40.1	43.4
		rubber object	1.3	8.6
red metal object	ViT	cube	0.2	11.1
		sphere	0.0	9.6

Table 3. **Complete table of experiments run in Section 4.1.** The explanations that obtained the highest CaCE for each classifier are shown in bold. In all cases except one, the rule used to train the target classifier was proposed by the LLM after Stage 3. The rule always corresponds to the hypothesis with the highest CaCE measurement. The use of italics for ‘red metal object’ indicates that the rule was manually created by recombining the first two rules found in Stage 3.

produced, which happens to be correct. Still, achieving high recall for hypotheses at this stage is crucial, as errors can be addressed during stage 4. Importantly, the rule always cor-

responds to the hypothesis with the highest CaCE measurement, ensuring a robust and systematic selection process.

Rule	Architecture	Explanation: ‘Class 1 contains a...’	Correct hypothesis
yellow rubber object	ViT	metal object	
metal object	ViT	metal object	✓
metal object	ResNet34	green object metal object red object and yellow object sphere and cube	✓
cyan object	ResNet34	blue sphere yellow or gray object	
cyan object	ViT	gray sphere yellow object	
purple object	ViT	purple object	✓
purple object	ResNet34	purple object purple sphere green object and purple object	✓
red metal object	ResNet34	red object yellow object red object and yellow object	
red metal object	ViT	red object metal object red object and metal object	
rubber object	ResNet34	yellow object green object metal object	
rubber object	ViT	blue object purple object yellow object and purple object red object and yellow object	

Table 4. **Ablation of Stage 2: Complete Output.** We replace the *change captions* with simple independently acquired *captions* for images and counterfactuals, using the prompt shown in Figure 14. The column ‘Correct hypothesis’ indicates whether the hypothesis corresponds to the rule used to train the classifier. The rule is found for only 4 out of the 12 classifiers tested. This ablation highlights the importance in our method of fine-grained pairwise comparisons between an image and its counterfactual explanation

Ablation of stage 2. Table 4 presents the results of stage 3 for the experiment in which we ablate the change captioning component (stage 2). In this experiment, the *change captions* are replaced with independently acquired *captions* for the images and their counterfactuals, using a prompt provided in Figure 14. This modification significantly reduces performance: the rule is correctly identified for only 4 out of the 12 classifiers tested. These results highlight the critical importance of fine-grained pairwise comparisons between an image and its counterfactual explanation. Such comparisons, facilitated by change captioning, are essential for the success of our method.

Number of Counterfactual Explanations (N). In our main experiment, we used a large number of counterfactuals, approximately $N = 100$ image pairs, as reported in the paper. This was our initial attempt, designed to ensure fairness without tuning the number of pairs. In the ablation study, we found that as few as three pairs ($N = 3$), and occasionally even two, were sufficient for the LLM to hypothesize the correct rule. This is because the change captioning stage (stage 2) is minimally noisy, as it uses CLIP4IDC, which is specifically trained for the image change captioning task. Additionally, the simplicity of the rule further reduces the need for a large number of counterfactual explanations.

E. Experimental Details on CelebA

E.1. GIFT Instantiation

The target model M is a DenseNet121 [39], trained to classify face images as either ‘old’ or ‘young,’ following prior work [40, 42].

For counterfactual generation (Stage 1), we leverage the diffusion-based model ACE [42], using its official implementation.

In the image change captioning stage (Stage 2), we employ Pixtral-12B VLM [3]. The prompt used for this stage is shown in Figure 13. To guide the VLM, we include a one-shot annotated sample within the prompt, where we manually describe the differences between a randomly selected image and its corresponding counterfactual explanation from stage 1. This guidance qualitatively improves the accuracy of the generated change captions.

Global explanation identification (Stage 3) is performed zero-shot using Qwen 2.5, a 72B parameter model, quantized to 8 bits [71]. The prompt used for this stage is provided in Figure 7.

For hypothesis verification and interventions in Stage 4, we use 200 images: 100 classified as ‘young’ and 100 classified as ‘old’ by the target classifier M .

- The VQA model for this stage is MiniCPM [84].
- Global interventions: For concepts that require global adjustments, such as increasing lighting, we use image-conditioned Stable Diffusion 3 [17].
- Local interventions: For concepts requiring localized changes, we first identify the region to be edited using Florence-2 [82] for open vocabulary detection. This provides the necessary masks, which are then passed to Stable Diffusion 2 [64], along with a prompt stating to add or remove the concept, resulting in the post-intervention image.

E.2. Results

Qualitative samples after stages 1 and 2. Figure 10 provides qualitative examples from stages 1 and 2 in the analysis of the CelebA ‘Young/Old’ classifier. The counterfactual explanations generated by ACE [42] highlight subtle changes, such as adding facial wrinkles or smoothing the skin. In stage 2, the Pixtral model produces detailed change captions that describe point-by-point differences between the original images and their corresponding counterfactual explanations. While most of the caption content is accurate and meaningful, we observe occasional noise and hallucinations from the VLM, where it describes changes that are not present in the images.

Complete results. Table 5 lists all the explanations associated with the class ‘Old,’ as generated by GIFT, along with

Explanations associated to the class ‘Old’	DI	CaCE
<i>after Stage 3</i>		
Receding Hairline	29.9	6.5
Neck Wrinkles	28.1	3.0
Wrinkles on Forehead	26.4	8.5
Wrinkles around Eyes	20.7	9.0
Glasses	16.5	10.5
Drooping Eyelids	15.4	5.5
Gray Hair	12.3	4.5
Small Eyes	3.6	
Thick Eyebrow	0.0	
Eyebrow Shape	2.1	
Prominent Cheekbones	0.7	
Visible Nasolabial Folds	0.6	
Prominent Jawline	0.6	
Pale Skin	0.8	
Serious Expression	0.1	
Dark Hair Color	0.0	
Long and Voluminous Hair	14.9	
Soft Lighting	0.2	
Detailed Background	0.2	
Tilted Head	0.3	
Low Camera Angle	0.1	
Prominent Ears	0.1	
Dark Facial Hair	2.8	
Tired-looking Eyes	13.4	
Pronounced Makeup	8.0	
Thin and Downturned Lips	5.0	
Wrinkles on Cheeks	11.9	
<i>after Stage 5</i>		
Gray Hair + Wrinkles around Eyes	39.1	7.8
Hairline + Wrinkles on Forehead	47.8	8.2
Glasses + Wrinkles around Eyes	60.4	21.7
Glasses + Wrinkles on Forehead	59.6	24.1
Glasses + Hairline	61.4	24.6
Glasses + Wrinkles on Forehead + Hairline	78.2	26.0
Glasses + Wrinkles on Forehead + Eyes	65.6	26.8

Table 5. Complete output of GIFT on the CelebA ‘Old’ classifier. DI and CaCE in %.

the corresponding DI and CaCE measurements. The identified attributes include plausible ones, such as ‘wrinkles on the forehead’ and ‘receding hairline,’ as well as more unexpected ones, such as a ‘detailed background’ or ‘low camera angle.’

F. Experimental Details on BDD-OIA bias discovery

F.1. GIFT Instantiation

The instantiation of GIFT for use-case 3, with the bias discovery, follows the same process as in the CelebA use-case,

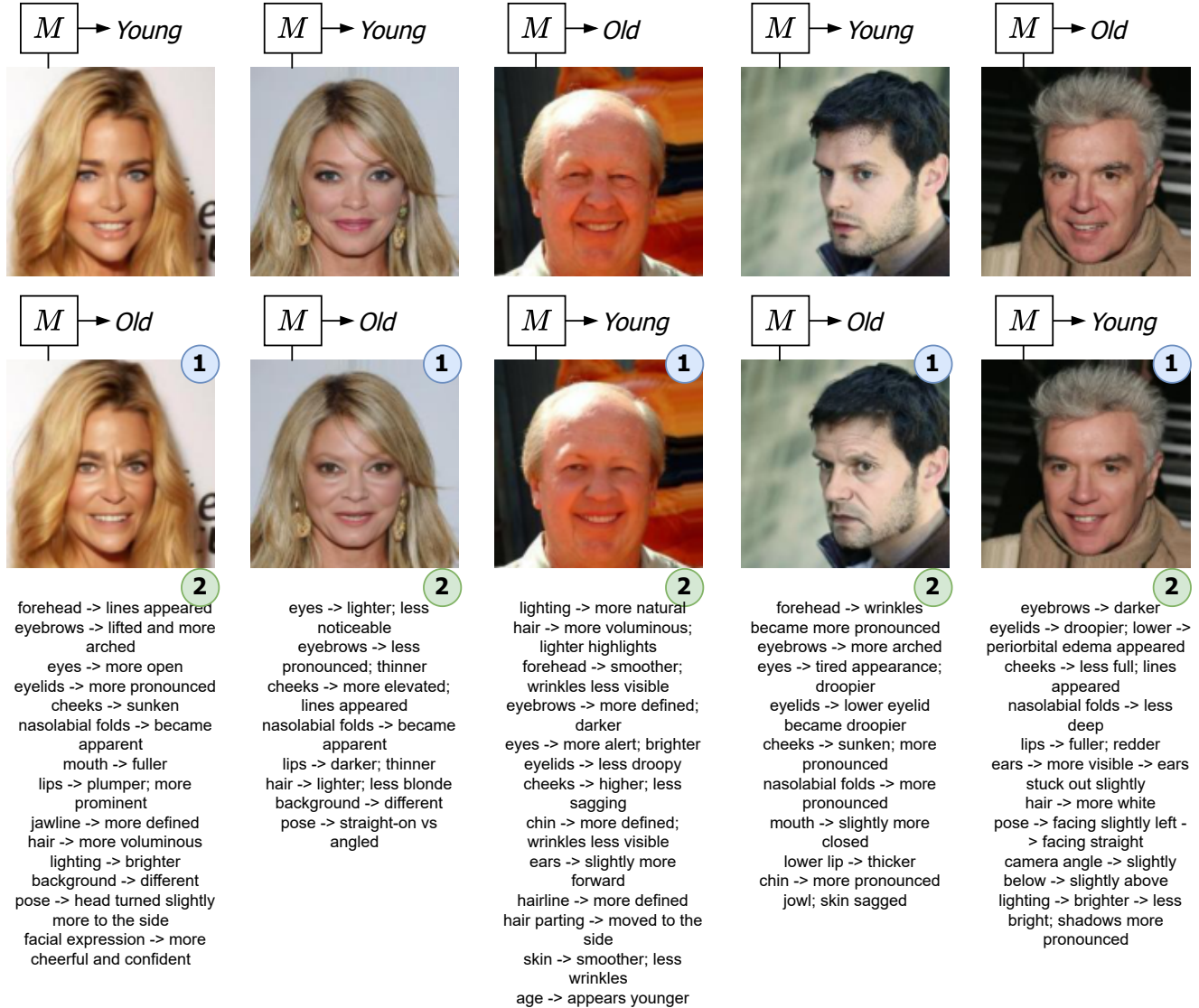


Figure 10. **Visualization of Stages 1 and 2 for the CelebA ‘Young/Old’ Classifier.** The top row shows the original images. The second row displays the corresponding counterfactual explanations generated in stage 1 using the diffusion-based ACE method [42]. The third row presents the change captions produced in stage 2 by the Pixtral model, which describe differences between the original images and their counterfactual explanations.

with the exception of counterfactual explanation generation. For this, we use OCTET [88], which comes with the BlobGAN [16] generative model for the BDD image domain. The biased ‘Turn right’ classifier used in OCTET serves as the target classifier for this use case.

F.2. Results

Qualitative samples after stages 1 and 2. Figure 11 provides qualitative examples from stages 1 and 2 in the analysis of the BDD-OIA ‘Can/Cannot turn right’ classifier. The counterfactual explanations generated by OCTET [42] highlight sparse semantic changes, despite significant pixel

value changes. This is due to the object-aware generative backbone, which manipulates disentangled representations of objects. For example, cars may appear or disappear (left and middle images) and shift their position, blocking lanes that were previously free. In stage 2, the VLM produces detailed change captions that describe the point-by-point differences between the original images and their corresponding counterfactual explanations. While most of the caption content is accurate, we observe occasional noise and hallucinations from the VLM, where it describes changes that are not actually present in the images.



Figure 11. **Visualization of the Stages 1 and 2** for the biased turn-right classifier trained on BDD-OIA data. The top row show original images. The second row show corresponding counterfactual explanations, obtained after stage 1 with OCTET [88]. The third row shows change captions that we obtain after stage 2, with the Pixtral change captioning.

Ablation of stage 2. In the baseline, described in Section 4.4 (‘Ablation of Stage 2’), instead of feeding the LLM with *change captions*, we provide simple captions for all images and counterfactuals. To generate the captions for each image, we use the recent Florence-2 [82], prompted with the ‘More detailed captions’ mode. Then, we feed all the captions, along with the classification yielded by the target model M , to the LLM, with a prompt shown in Figure 14. LLM fails to hypothesize that Class ‘1’ is confounded by the presence of vehicles in the left lane. This ablation highlights the importance of fine-grained pairwise comparisons between an image and its counterfactual explanation, as provided by stage 2, are crucial for the effectiveness of our method.

Ablation of stages 1 and 2. In the baseline, described in Section 4.4 (‘Ablation of Stages 1 and 2’), we prompt the LLM of Stage 3 to imagine possible biases that the target classifier may suffer. There are thus no counterfactual explanations generation and the LLM does not depend

on any information given by the classifier, except for the class meaning (=labels). We show the prompt and output in Figure 15. As there are no dependencies anymore on the target classifier, the LLM can only imagine generic biases and fails to find the unexpected left-lane bias. As LLM-generated hypotheses fail to raise the left-lane-vehicle bias, it shows the importance of the counterfactual guidance (stages 1 and 2) in the GIFT framework

Number of counterfactual explanations N . Our main experiment used a large number of counterfactuals, approximately 150 image pairs, as reported in the paper. This was our initial attempt, without tweaking this number, to ensure fairness. We then conducted an ablation study to determine the minimum number of pairs needed to detect the bias. The results showed that at least 20 pairs are required to reliably identify the bias. The key insights are: using a large number of pairs works well, as the LLM is able to reason effectively and filter out noise. We hypothesize that a smaller LLM might struggle in this scenario. Additionally, unlike

CLEVR, where only three pairs were sufficient, the noisier change captions in this case require more pairs to allow the LLM to distinguish the true signal from the noise.

G. Limitations

As GIFT builds on various models from recent literature, it inherits the limitations of its components. Below, we discuss these limitations and propose potential ways to address them in future work.

Scope of counterfactual explanations (Stage 1). The scope of counterfactual explanations is constrained by the generative model underlying the counterfactual method. Methods like STEEX [40] and ACE [42] limit the search space and, for instance, cannot assess the importance of object positions. OCTET [88], which uses BlobGAN [16], offers a partial solution by enabling disentangled representations of scene layout and semantics ; this motivates our choice of OCTET for object-centric datasets (CLEVR in Section 4.1 and BDD in Section 4.3).

To mitigate the potentially limiting scope of the counterfactual explanation method, combining multiple counterfactual methods could improve the diversity and completeness of the explanations. Despite these constraints, our results show that grounding the explanations in local counterfactuals reveals unexpected biases and insights that human- or LLM-generated hypotheses might miss (Section 4.4).

Image change captioning in complex domains (Stage 2). Stage 2 relies on an image change captioning model, which face challenges in new and complex domains, such as driving scenes. These models often lack the training to interpret domain-specific or fine-grained changes, such as precise object positions or subtle attributes, which require an advanced understanding of compositional scene structure [53, 61].

A potential solution is to generate synthetic perturbations using models like InstructPix2Pix [10]. This method creates triplets of original images, edited images, and captions that could be used to fine-tune vision-language models for more accurate change captioning in specific domains.

Reasoning capabilities of the LLM (Stage 3). Stage 3 leverages an LLM to identify global explanations from noisy change captions. This requires the LLM to disambiguate local evidence and infer common explanations across multiple counterfactual changes (as explained in Section 3.4). Although our experiments show that LLMs perform reasonably well in this task, it remains an unconventional use case for the LLM.

Future work could explore fine-tuning LLMs specifically for this task to improve their ability to reason over aggre-

gated counterfactual signals and handle more complex scenarios.

Text-guided image editing for fine-grained queries (Stage 4). Text-guided image editing (Stage 4) can produce unrealistic outputs, particularly for complex scenes or fine-grained, compositional queries like "Shift the red car on the right of the black truck to left" [53, 61]. While recent advances in compositional understanding [17] show promise, further progress is needed to handle such detailed queries reliably.

Automated exploration of the explanation space (Stage 5). Stage 5 allows users to explore and combine concepts with observed correlation or causal signals or to test their own hypotheses. While this human-in-the-loop approach is desirable as it implies end-users in the process, fully automating the exploration process could enhance scalability.

One promising direction involves using the Stage 3 LLM to iteratively reason over counterfactual descriptions while incorporating feedback from correlation (DI) and causal measurements (CaCE). This could follow the 'visual programming' paradigm [33], where the LLM utilizes tools like Stage 4 verification in a chain-of-thought manner [80]. However, our initial experiments in this direction were unsatisfactory, highlighting the current limitations of LLM reasoning for such ambitious goals.

You are an expert in street/road traffic analysis and driving-scene analysis.

[INST] List how Image-2 differs from Image-1:

- Consider how each element of the image (objects, people, animals, etc.) has changed, considering their sizes, materials, colors, textures, poses, positions, and relative positions
- Consider elements that might have appeared or disappeared in the transition to Image-2 from Image-1
- Consider whether the image or scene as a whole has changed, and if that's the case, explain how
- Omit commonalities; focus only on the differences
- BE RIGOROUS: DO include comparisons that are clearly visible in both images; DO NOT guess or infer details
- Present the changes as a plain-text list, one change per line, in the format <element> → [<specifics> →] → <change>

[/INST]

—
Image-1: IMAGE_TOKEN

—
Image-2: IMAGE_TOKEN

—
CHANGES:

road → left lane → was clear, now blocked by a car in the same direction
road → right lane → had an incoming car, now has car in the same direction
road → middle lane → surface more reflective
road → pedestrian crossing → less visible; more faded
traffic lights → leftmost → appeared; green light
middle car → brighter; color more saturated
rightmost streetlight → disappeared
ego-car → dashboard → brighter

—
Image-1: IMAGE_TOKEN

—
Image-2: IMAGE_TOKEN

—
CHANGES:

Figure 12. **Prompts used for stage 2 for BDD.** We prompt the Pixtral VLM for the image change captioning stage. The special tokens 'IMAGE_TOKEN' are replaced by the tokenized images. We use a one-shot in-prompt annotated sample as guidance, where we manually describe the differences between an image (randomly selected) and the obtained counterfactual explanation after stage 1.

You are an expert in image analysis and forensic facial comparison.

[INST] List how Image-2 differs from Image-1:

- Consider how each facial feature has changed, including the eyes, nose, mouth, ears, hair, etc
- Consider whether the facial expression has changed and how this has affected the facial appearance
- Consider whether the pose and camera angle have changed
- Consider whether the lighting, background, and other environmental factors have changed
- Omit commonalities; focus only on the differences
- BE RIGOROUS: DO include comparisons that are clearly visible in both images; DO NOT guess or infer details
- Present the changes as a plain-text list, one change per line, in the format <element> → [<specifics> →] → <change>

[/INST]

—
Image-1: IMAGE_TOKEN

—
Image-2: IMAGE_TOKEN

—
CHANGES:

forehead → lines appeared
eyes → darker; less shiny
eyelids → lower → periorbital edema appeared
cheeks → more prominent; lines appeared
nose → slightly wider
nasolabial folds → became apparent; very marked
lips → thinner; darker; less red

—
Image-1: IMAGE_TOKEN

—
Image-2: IMAGE_TOKEN

—
CHANGES:

Figure 13. **Prompts used for stage 2 for CelebA.** We prompt the Pixtral VLM for the image change captioning stage. The special tokens ‘IMAGE_TOKEN’ are replaced by the tokenized images. We use a one-shot in-prompt annotated sample as guidance, where we manually describe the differences between an image (randomly selected) and the obtained counterfactual explanation after stage 1.

Each one of the descriptions below (separated by ‘—’) details the content of an image. The descriptions are grouped by the prediction of a binary classifier on their corresponding images: images classified as 0 and images classified as 1. Your task is to consider ALL the descriptions and identify the main factors that could lead the classifier to choose class 0 over class 1, and vice-versa.

The set of description is noisy, and the descriptions may contain irrelevant or contradictory information. Your task is to focus on the most important factors that appear consistently across many instances

-Find testable factors that can be observed and measured in the images (e.g., objects’ presence, appearance, arrangement, etc.)

-Present your factors as a bulleted list

Description of images classified as 0:

—

The image is of a highway at night. The sky is dark and the street lights are on. There are two yellow lines painted on the road. On both sides of the road there are rows of parked cars. The cars are all black in color. In the front of the image there is a windshield of a car. The headlights of the cars are on and they are all turned on.

—

Cars are driving on a street at night. The street has white lines on it. There are buildings on both sides of the street. The sky is dark and there are street lights on.

—

...

Description of images classified as 1:

—

A car is driving down the street. There are several cars parked on the side of the street next to tall buildings. There is a red car in the middle of the road.

—

This is an image of a highway at night. The sky is completely black. The street lights are on. There are two yellow lines painted on the road. There is a red car in the middle of the street. The headlights of the car are on and it is dark outside. The car is driving on the right side of the road and there are several other cars on the left side.

—

A car is driving down the street at night. There are white lines painted on the street. There is a green light in the distance on the road.

...

—

[Answer]

- Street Lines and Markings: More detailed and frequent in class 0.
- Parked Cars: More common in class 0.
- Building Appearance: More detailed and diverse in class 1.
- Lighting and Reflections: Brighter and more reflective in class 1.
- Time of Day: More night time in class 0, more varied in class 1.
- Traffic Density: Higher in class 1.
- Perspective: More inside car in class 0, more varied in class 1

Figure 14. **Ablation of Stage 2: Prompt and LLM Response in Stage 3.** The top section shows the prompt used to query the LLM, where we provide Florence-2-generated captions for all images and their counterfactuals, grouped according to the classification outcomes of the target model. Class ‘0’ corresponds to *Cannot turn right*, and Class ‘1’ corresponds to *Can turn right*. The bottom section displays the LLM’s response. Notably, the LLM fails to hypothesize that Class ‘1’ is confounded by the presence of vehicles in the left lane. This ablation highlights the importance of fine-grained pairwise comparisons between an image and its counterfactual explanation, which are crucial for the effectiveness of our method.

[Prompt] :

You are an expert in analyzing and explaining the behavior of machine learning classifiers. Consider a binary classifier designed to predict whether a vehicle in a driving scene can turn right. This classifier is potentially imperfect. What possible biases or spurious correlations might this classifier have regarding the decision to turn right?

[Answer by Qwen 2.5] :

- Time of Day: The classifier might learn that certain times of day (e.g., rush hour) are more likely to have restrictions on turning right due to increased traffic.
 - Day of the Week: Similar to time of day, the classifier might pick up on patterns where certain days (e.g., weekends vs. weekdays) have different traffic conditions that affect the ability to turn right.
 - Urban vs. Rural Areas: The classifier might learn that turning right is more common or less restricted in rural areas compared to urban areas due to differences in traffic density and infrastructure.
 - Specific Locations: The classifier might overfit to specific intersections or regions where turning right is either very common or very rare, leading to poor generalization to new locations.
 - Weather Patterns: The classifier might learn that certain weather conditions (e.g., rain, snow) make it less likely for vehicles to turn right due to reduced visibility or road conditions.
 - Type of Vehicle: The classifier might pick up on correlations between the type of vehicle (e.g., trucks, cars, motorcycles) and the likelihood of turning right. For example, larger vehicles might be less likely to turn right in tight spaces.
 - Traffic Light States: The classifier might learn that certain states of traffic lights (e.g., red light) are associated with not being able to turn right.
 - Signage: The presence or absence of specific traffic signs (e.g., "No Right Turn" signs) might be overemphasized by the classifier.
 - Driver Demographics: If the dataset includes information about the driver, the classifier might pick up on spurious correlations related to the age, gender, or experience level of the driver.
 - Driver Intent: The classifier might infer the driver's intent to turn right based on subtle cues that are not directly related to the feasibility of the turn (e.g., the position of the turn signal).
 - Dataset Imbalance: If the dataset contains a disproportionate number of examples where turning right is allowed or prohibited, the classifier might be biased towards the more frequent class.
 - Sensor Quality: Differences in the quality or type of sensors used to collect data (e.g., cameras, LIDAR) might introduce biases if the classifier learns to rely on artifacts specific to certain sensor types.
 - Overfitting to Training Data: The classifier might overfit to the specific characteristics of the training data, leading to poor performance on unseen data. This can manifest as spurious correlations that do not generalize well.
 - Pedestrian Presence: The classifier might learn that the presence of pedestrians near the intersection makes it less likely to turn right.
 - Bicycle Lanes: The presence of bicycle lanes might be correlated with restrictions on turning right, especially in areas with high bicycle traffic.
-

Figure 15. **Ablation of stages 1 and 2 on BDD-OIA bias discovery.** In this experiment, we prompt the LLM in Stage 3 to imagine possible biases that the target classifier may have (prompt shown at the top), and display the LLM's response (bottom). Without relying on the target classifier, the LLM only generates generic biases and fails to detect the unexpected left-lane bias. This demonstrates the critical role of counterfactual guidance (stages 1 and 2) in the GIFT framework.